

Hypnozoite dynamics for *Plasmodium vivax* malaria: the epidemiological effects of radical cure

Somya Mehra¹ Eva Stadler² David Khoury² James M. McCaw^{1,3,4}
Jennifer A. Flegg¹

¹School of Mathematics and Statistics, The University of Melbourne, Parkville, Australia

²Kirby Institute, University of New South Wales, Kensington, Australia

³Centre for Epidemiology and Biostatistics, Melbourne School of Population and Global Health, The University of Melbourne, Parkville, Australia

⁴Peter Doherty Institute for Infection and Immunity, The Royal Melbourne Hospital and The University of Melbourne, Parkville, Australia

Abstract

Malaria is a mosquito-borne disease with a devastating global impact. *Plasmodium vivax* is a major cause of human malaria beyond sub-Saharan Africa. Relapsing infections, driven by a reservoir of liver-stage parasites known as hypnozoites, present unique challenges for the control of *P. vivax* malaria. Following indeterminate dormancy periods, hypnozoites may activate to trigger relapses. Clearance of the hypnozoite reservoir through drug treatment (radical cure) has been proposed as a potential tool for the elimination of *P. vivax* malaria. Here, we introduce a stochastic, within-host model to jointly characterise hypnozoite and infection dynamics for an individual in a general transmission setting, allowing for radical cure. We begin by extending an existing activation-clearance model for a single hypnozoite, adapted to both short- and long-latency strains, to include drug treatment. We then embed this activation-clearance model in an epidemiological framework accounting for repeated mosquito inoculation and the administration of radical cure. By constructing an open network of infinite server queues, we derive analytic expressions for several quantities of epidemiological significance, including the size of the hypnozoite reservoir; the relative contribution of relapses to the infection burden; the distribution of multiple infections; the cumulative number of recurrences over time, and the time to first recurrence following drug treatment. By deriving, rather than assuming parame-

teric forms, we characterise the transient dynamics of the hypnozoite reservoir following radical cure more accurately than previous approaches. To yield population-level insights, our analytic within-host distributions can be embedded in multiscale models. Our work thus contributes to the epidemiological understanding of the effects of radical cure on *P. vivax* malaria.

1 Introduction

Malaria remains a significant cause of morbidity and mortality, with an estimated 229 million cases and 409,000 deaths in 2019 alone (WHO 2020). *Plasmodium falciparum* and *Plasmodium vivax*, which are transmitted to humans through the bites of infected *Anopheles* mosquitoes, are the primary contributors to the global malaria burden. While the prevalence of *P. falciparum* remains higher than that for *P. vivax* globally, the relative burden of *P. vivax* has increased in various co-endemic settings as malaria elimination efforts have intensified (Price et al. 2020).

The control and elimination of *P. vivax* malaria is complicated by various biological characteristics of both parasite and vector (WHO 2015; Howes et al. 2016; Olliaro et al. 2016; Price et al. 2020). Relapsing infections, driven by a reservoir of latent liver-stage parasites known as hypnozoites, are perhaps the key distinguishing feature of *P. vivax*. For vivax malaria, each infective bite can trigger a primary (blood-stage) infection, in addition to establishing a variable hypnozoite inoculum (White and Imwong 2012). Hypnozoites remain inactive and undetectable in the liver for indeterminate periods, with long-latency phenotypes typically observed in temperate regions, and short-latency phenotypes generally observed in tropical regions (White and Imwong 2012; Battle et al. 2014). Each hypnozoite activation event, however, has the potential to trigger a new blood-stage infection, called a relapse. The hypnozoite reservoir can thus re-establish transmission within a community, even after the elimination of all active infections (Shanks 2012).

Although the clearance of the hypnozoite reservoir is critical to elimination efforts, the majority of antimalarial drugs exclusively target the blood-stages of infection. Only a small class of drugs have hypnozoiticidal activity; such treatments are collectively referred to as radical cure because of their ability to eliminate both active and latent parasites (Wells, Burrows, and Baird 2010). Radical cure has been proposed as a potential tool for *P. vivax* malaria elimination (Shanks 2012). However, the widespread adoption of radical cure treatments has been curtailed, largely because of the risk of haemolysis in G6PD deficient individuals (Wells, Burrows, and Baird 2010; WHO 2015). Here, we develop a mathematical model of the dynamics of the hypnozoite

reservoir within a single host in a general transmission setting to explore the epidemiological consequences of radical cure.

Previous simulation models of within-host *P. vivax* dynamics have examined the complexities of hypnozoite activation and blood-stage infection, but have not considered the accrual of the hypnozoite reservoir in endemic settings (Kerlin and Gatton 2015). Transmission models accounting for individuals carrying hypnozoites have been developed, but have generally compartmentalised individuals carrying at least one hypnozoite, without explicitly modelling the size of the hypnozoite reservoir (Ishikawa et al. 2003; Aguas, Ferreira, and Gomes 2012; Roy et al. 2013; Chamchod and Beier 2013; Robinson et al. 2015; White, Shirreff, et al. 2016). Various distributional forms for the time-to-relapse, including exponential distributions (Aguas, Ferreira, and Gomes 2012; Chamchod and Beier 2013; Robinson et al. 2015; White, Shirreff, et al. 2016), log-normal distributions (Ishikawa et al. 2003), gamma distributions (Roy et al. 2013) and mixture distributions (Lover et al. 2014; Taylor et al. 2019), have been assumed without accounting for the dependency between the size of the hypnozoite reservoir and the risk of relapse. Transmission models accounting for the accrual of the hypnozoite reservoir over successive mosquito bites, in addition to immunity, prophylaxis and clinical symptoms, have been proposed by White, Walker, et al. (2018); yet, in assuming that each batch of hypnozoites (established by the same mosquito bite) gives rise to relapses at the same constant rate, these models do not account for variability in parasite inocula across bites, which can modulate the risk of relapse (White and Imwong 2012). By embedding a within-host model of hypnozoite activation in a population-level transmission model accounting for variability in hypnozoite inocula, White, Karl, et al. (2014) have obtained distributions for the prevalence of vivax malaria and the size of the hypnozoite reservoir under a range of control interventions, including radical cure. However, distributions of multiple infections; the relative contributions of primary infections to the infection burden; and the cumulative number of relapses over time have not been examined in this framework, which has moreover been restricted to short-latency strains (White, Karl, et al. 2014).

In this paper, we develop a within-host model to jointly characterise the accrual of the hypnozoite reservoir and the infection burden over time, whilst accounting for drug treatment, for both short- and long-latency strains. In Section 2, we extend an existing activation-clearance model for a single hypnozoite (White, Karl, et al. 2014; Mehra et al. 2020) to consider treatment with blood-stage (schizontocidal) drugs and radical cure. To characterise the dynamics of the hypnozoite reservoir and blood-stage infections in an endemic setting, we then embed this activation-clearance model in an epidemiological framework in Section 3, extending our

previous work (Mehra et al. 2021) to account for drug treatment. By constructing an open network of infinite server queues, we derive a joint probability generating function (PGF) for the number of hypnozoites in each state of the model, in addition to the number of cleared and ongoing recurrences, for an individual in a general transmission setting. In Section 4, we derive analytic expressions for quantities of epidemiological significance, including the size of the hypnozoite reservoir; the risk of primary infections and relapses over time; the incidence of multiple infections; the time to first recurrence following drug treatment and the cumulative number of recurrences in a given interval. To capture the epidemiological effects of radical cure, we compare hypnozoite and infection dynamics following treatment with radical cure against a scenario with no treatment or blood-stage treatment only, with illustrative results provided and discussed in Section 5 and concluding remarks in Section 6.

2 Relapse-Clearance Dynamics for a Single Hypnozoite

2.1 Baseline Scenario

We begin by developing a model of relapse-clearance dynamics for a single hypnozoite in a baseline scenario, neither accounting for drug treatment nor external triggers of hypnozoite activation. Similarly to White, Karl, et al. (2014), we assume that each hypnozoite undergoes a dormancy phase, during which it can die, but not activate. We model this dormancy phase as a series of $k \geq 0$ compartments, with transition rate δ between compartments. Hypnozoites that have emerged from dormancy (hereafter referred to as non-latent hypnozoites) are assumed to activate at some constant rate α . We also assume that all hypnozoites in the liver (that is, both dormant and non-latent hypnozoites) are subject to death at constant rate μ , potentially due to the death of the host hepatocyte. This activation-clearance model was introduced in White, Karl, et al. (2014) and discussed in detail in Mehra et al. (2020), along with analytic solutions to the state probabilities. Here, we further assume that hypnozoite activation immediately triggers a blood-stage infection (relapse) that is cleared at rate γ (that is, exponentially-distributed with expected duration $1/\gamma$). Each hypnozoite therefore has two possible end states: death prior to activation, or clearance following blood-stage infection. A schematic of this model structure is shown in Figure 1.

The case $k > 0$ captures hypnozoite dynamics for long-latency (temperate) strains of *P. vivax*. By setting $k = 0$, that is, accounting for a scenario where each hypnozoite may activate immediately after it is established in the liver, we recover a model for short-latency (tropical) strains

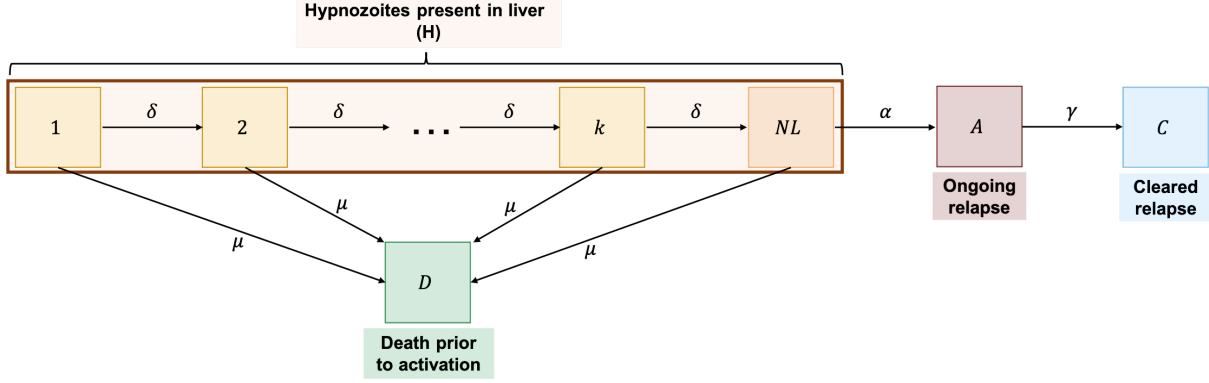


Figure 1: Schematic for relapse-clearance model of a single hypnozoite under a baseline scenario, in the absence of drug treatment or external triggers of hypnozoite activation. States $1, \dots, k$ denote latency compartments; NL denotes a non-latent hypnozoite; D denotes a hypnozoite that has died prior to activation; A denotes an ongoing relapse triggered by hypnozoite activation and C denotes a relapse that has been cleared from the bloodstream. State H collectively refers to hypnozoites that are present in the liver, that is, both non-latent (NL) and latent ($1, \dots, k$) hypnozoites. Setting $k = 0$ captures the dynamics of short-latency (tropical) strains, while $k > 0$ applies to long-latency (temperate) strains (White, Karl, et al. 2014).

(White, Karl, et al. 2014).

Suppose that a single hypnozoite is established in a host hepatocyte at time zero. Denote the state of the hypnozoite at time t by $X(t)$. Then $X(t)$ has probability mass function (PMF)

$$\mathbf{p}(t) = (p_1(t), \dots, p_k(t), p_{NL}(t), p_A(t), p_C(t), p_D(t))$$

where the state probabilities are defined to be

- $p_m(t)$ that the hypnozoite is present in latency compartment $m \in [1, k]$ at time t ;
- $p_{NL}(t)$ that a hypnozoite is non-latent, that is, present in the liver and may activate, at time t (state NL);
- $p_A(t)$ that the hypnozoite has activated and triggered a relapse that is ongoing at time t (state A);
- $p_C(t)$ that the hypnozoite has activated to cause a relapse that has been cleared by time t (state C);
- $p_D(t)$ that the hypnozoite has died prior to activating by time t (state D).

For notational convenience, we define

$$p_H(t) = \sum_{m=1}^k p_m(t) + p_{NL}(t)$$

to be the probability that a hypnozoite is present in the liver, that is, state H , at time t .

Based on the model schematic in Figure 1 and the Kolmogorov forward differential equations, it follows that

$$\frac{dp_1}{dt} = -(\delta + \mu)p_1(t) \quad (1)$$

$$\frac{dp_m}{dt} = -(\delta + \mu)p_m(t) + \delta p_{m-1}(t), \quad m \in [2, k] \quad (2)$$

$$\frac{dp_{NL}}{dt} = -(\alpha + \mu)p_{NL}(t) + \delta p_k(t) \quad (3)$$

$$\frac{dp_A}{dt} = -\gamma p_A(t) + \alpha p_{NL}(t) \quad (4)$$

$$\frac{dp_C}{dt} = \gamma p_A(t) \quad (5)$$

$$\frac{dp_D}{dt} = \mu \sum_{i=1}^k p_i(t) + \mu p_{NL}(t) = \mu p_H(t), \quad (6)$$

with the initial condition

$$\mathbf{p}(0) = \begin{cases} (p_1(0), p_2(0), \dots, p_k(0), p_{NL}(0), p_A(0), p_C(0), p_D(0)) = (1, 0, \dots, 0, 0, 0, 0, 0) & \text{if } k > 0 \\ (p_{NL}(0), p_A(0), p_C(0), p_D(0)) = (1, 0, 0, 0) & \text{if } k = 0 \end{cases} \quad (7)$$

Integrating by parts, we can solve the system in Equations (1) to (6), subject to initial condition

(7) to yield

$$p_m(t) = \frac{(\delta t)^{m-1}}{(m-1)!} e^{-(\mu+\delta)t} \text{ for } m \in [1, k] \quad (8)$$

$$p_{NL}(t) = \frac{\delta^k}{(\delta - \alpha)^k} \left[e^{-(\mu+\alpha)t} - e^{-(\mu+\delta)t} \sum_{j=0}^{k-1} \frac{t^j}{j!} (\delta - \alpha)^j \right] \quad (9)$$

$$p_A(t) = \frac{\alpha \delta^k}{(\delta - \alpha)^k} \left[\frac{e^{-(\mu+\delta)t}}{\mu - \gamma + \delta} \left\{ \sum_{j=0}^{k-1} \left(\frac{\delta - \alpha}{\mu - \gamma + \delta} \right)^j \sum_{i=0}^j \frac{t^i}{i!} (\mu - \gamma + \delta)^i \right\} - \frac{e^{-(\mu+\alpha)t}}{\mu - \gamma + \alpha} \right] + \frac{\alpha}{\alpha + \mu - \gamma} \left(\frac{\delta}{\delta + \mu - \gamma} \right)^k e^{-\gamma t} \quad (10)$$

$$p_C(t) = \frac{\alpha}{\alpha + \mu} \left(\frac{\delta}{\mu + \delta} \right)^k - \frac{\alpha}{\alpha + \mu - \gamma} \left(\frac{\delta}{\delta + \mu - \gamma} \right)^k e^{-\gamma t} + \frac{\gamma \alpha \delta^k}{(\delta - \alpha)^k} \frac{e^{-(\mu+\alpha)t}}{(\mu + \alpha)(\mu - \gamma + \alpha)} - \frac{\gamma \alpha \delta^k}{(\delta - \alpha)^k} \frac{e^{-(\mu+\delta)t}}{(\mu - \gamma + \delta)(\mu + \gamma)} \left\{ \sum_{j=0}^{k-1} \left(\frac{\delta - \alpha}{\mu - \gamma + \delta} \right)^j \sum_{i=0}^j \left(\frac{\mu - \gamma + \delta}{\mu + \delta} \right)^i \sum_{q=0}^i \frac{t^q}{q!} (\mu + \delta)^q \right\} \quad (11)$$

$$p_D(t) = 1 - \sum_{m=1}^k p_m(t) - p_{NL}(t) - p_A(t) - p_C(t), \quad (12)$$

where we have used standard integral number 2.321.2 in Jeffrey and Zwillinger (2007). For a physical interpretation of the activation-clearance system for long-latency strains, which accounts for hypnozoite death, dormancy and activation, but does not account for the clearance of relapses (that is, does not distinguish states A and C), see Mehra et al. (2020).

In the case $k = 0$, corresponding to short-latency (tropical) strains, whereby all hypnozoites in the liver may activate, Equations (9) to (12) simplify to

$$p_H(t) = p_{NL}(t) = e^{-(\alpha+\mu)t} \quad (13)$$

$$p_A(t) = \frac{\alpha}{(\alpha + \mu) - \gamma} (e^{-\gamma t} - e^{-(\alpha+\mu)t}) \quad (14)$$

$$p_C(t) = \frac{\alpha}{\alpha + \mu} (1 - e^{-(\alpha+\mu)t}) - \frac{\alpha}{(\alpha + \mu) - \gamma} (e^{-\gamma t} - e^{-(\alpha+\mu)t}) \quad (15)$$

$$p_D(t) = \frac{\mu}{\alpha + \mu} (1 - e^{-(\alpha+\mu)t}). \quad (16)$$

2.2 Drug Treatment

We now extend the baseline model introduced in Section 2.1 to account for drug treatment. We make the simplifying approximation that drug treatment has an instantaneous effect; while antimalarial drug half-lives vary broadly, from approximately 40 minutes for artesunate (Morris

et al. 2011), to 6 hours for primaquine (radical cure) (White 1992) and 30-60 days for chloroquine (White 1992), we are primarily concerned with hypnozoite dynamics over a time frame of years, and therefore this assumption of instantaneous action is appropriate. Upon administration of drug treatment, we thus assume that each hypnozoite in the liver (that is, states $1, \dots, k, NL$, collectively referred to as state H) dies instantaneously (that is, transitions to state D) with probability p_{rad} ; while any ongoing blood-stage infections (that is, hypnozoites in state A) are instantaneously cleared (that is, transition to state C) with probability p_{blood} . The case $p_{\text{blood}} > 0, p_{\text{rad}} = 0$ corresponds to blood-stage treatment only, while $p_{\text{blood}} > 0, p_{\text{rad}} > 0$ corresponds to hypnozoiticidal treatment (radical cure). Any hypnozoites that survive radical cure (that is, remain in state H) or persisting blood-stage infections (state A) are then subject to the same activation-clearance dynamics described in Section 2.1.

Consider a single hypnozoite inoculated at time $t = 0$. Suppose that drug treatment is administered successively at times s_1, s_2, \dots, s_n . We denote the state of the hypnozoite at time t $X^r(t, s_1, \dots, s_n) \in \{1, \dots, k, NL, A, C, D\}$ with corresponding PMF $\mathbf{p}^r(t, s_1, \dots, s_n)$. The governing equations for the state probabilities are given by:

$$\frac{dp_1^r}{dt} = -(\delta + \mu)p_1^r - \ln((1 - p_{\text{rad}})^{-1}) \sum_{j=1}^n \delta_D(t - s_j)p_1^r \quad (17)$$

$$\frac{dp_m^r}{dt} = -(\delta + \mu)p_m^r + \delta p_{m-1}^r - \ln((1 - p_{\text{rad}})^{-1}) \sum_{j=1}^n \delta_D(t - s_j)p_m^r, \quad m \in [2, k] \quad (18)$$

$$\frac{dp_{NL}^r}{dt} = -(\alpha + \mu)p_{NL}^r + \delta p_k^r - \ln((1 - p_{\text{rad}})^{-1}) \sum_{j=1}^n \delta_D(t - s_j)p_{NL}^r \quad (19)$$

$$\frac{dp_A^r}{dt} = -\gamma p_A^r + \alpha p_{NL}^r - \ln((1 - p_{\text{blood}})^{-1}) \sum_{j=1}^n \delta_D(t - s_j)p_A^r \quad (20)$$

$$\frac{dp_C^r}{dt} = \gamma p_A^r + \ln((1 - p_{\text{blood}})^{-1}) \sum_{j=1}^n \delta_D(t - s_j)p_A^r \quad (21)$$

$$\frac{dp_D^r}{dt} = \mu \left(\sum_{i=1}^k p_i^r + p_{NL}^r \right) + \ln((1 - p_{\text{rad}})^{-1}) \sum_{j=1}^n \delta_D(t - s_j) \left(\sum_{i=1}^k p_i^r + p_{NL}^r \right), \quad (22)$$

where $\delta_D(\cdot)$ denotes the Dirac delta function (not to be confused with δ , a scalar parameter that denotes the rate of transition between successive latency compartments).

Here, we restrict our attention to a single administration of drug treatment at time s_1 . For $t < s_1$, we note that $\mathbf{p}^r(t, s_1) = \mathbf{p}(t)$, as per Equations (8) to (12). Since we model the effects of radical cure to be instantaneous, $\mathbf{p}^r(t, s_1)$ will exhibit jump discontinuities at time $t = s_1$.

Integrating by parts, we can solve Equations (17) to (22) for $t \geq s_1$ to obtain the state probabilities $\mathbf{p}^r(t, s_1)$ in terms of the state probabilities $\mathbf{p}(t)$ given by Equations (8) to (12):

$$p_m^r(t, s_1) = \underbrace{(1 - p_{\text{rad}}) \cdot p_m(t)}_{\substack{\text{radical cure failure: hypnozoite} \\ \text{(dormant) survives treatment at } s_1}} \quad \text{for } m \in [1, k] \quad (23)$$

$$p_{NL}^r(t, s_1) = \underbrace{(1 - p_{\text{rad}}) \cdot p_{NL}(t)}_{\substack{\text{radical cure failure: hypnozoite} \\ \text{(non-latent) survives treatment at } s_1}} \quad (24)$$

$$p_A^r(t, s_1) = \underbrace{(1 - p_{\text{blood}})e^{-\gamma(t-s_1)}p_A(s_1)}_{\substack{\text{blood-stage treatment failure:} \\ \text{drug fails to clear infection at } s_1}} + \underbrace{(1 - p_{\text{rad}})(p_A(t) - e^{-\gamma(t-s_1)}p_A(s_1))}_{\substack{\text{relapse triggered by a hypnozoite that survives} \\ \text{drug treatment at } s_1 \text{ (i.e. radical cure failure)}}} \quad (25)$$

$$p_C^r(t, s_1) = \underbrace{p_C(s_1)}_{\substack{\text{relapse cleared} \\ \text{naturally} \\ \text{before } s_1}} + \underbrace{p_{\text{blood}} \cdot p_A(s_1)}_{\substack{\text{blood-stage treatment success:} \\ \text{drug instantaneously clears} \\ \text{ongoing infection at } s_1}} + \underbrace{(1 - p_{\text{blood}})(1 - e^{-\gamma(t-s_1)})p_A(s_1)}_{\substack{\text{relapse surviving drug treatment at } s_1 \\ \text{(i.e. blood-stage treatment failure)} \\ \text{is later cleared naturally}}} + \underbrace{(1 - p_{\text{rad}})[p_C(t) - p_C(s_1) - (1 - e^{-\gamma(t-s_1)})p_A(s_1)]}_{\substack{\text{relapse triggered by a hypnozoite that survives} \\ \text{drug treatment at } s_1 \text{ (i.e. radical cure failure)} \\ \text{is later cleared naturally}}} \quad (26)$$

$$p_D^r(t, s_1) = \underbrace{p_D(s_1)}_{\substack{\text{hypnozoite dies} \\ \text{naturally} \\ \text{before } s_1}} + p_{\text{rad}} \cdot \underbrace{\left(\sum_{m=1}^k p_m(s_1) + p_{NL}(s_1) \right)}_{\substack{\text{radical cure success: hypnozoite} \\ \text{(dormant or non-latent) instantaneously} \\ \text{killed by drug at } s_1}} + \underbrace{(1 - p_{\text{rad}})[p_D(t) - p_D(s_1)]}_{\substack{\text{hypnozoite surviving treatment at } s_1 \\ \text{(i.e. radical cure failure)} \\ \text{later dies naturally}}} \quad (27)$$

Illustrative results for our activation-clearance model, comparing blood-stage treatment only ($p_{\text{blood}} = 1$, $p_{\text{rad}} = 0$) against reasonably efficacious radical cure ($p_{\text{blood}} = 1$, $p_{\text{rad}} = 0.95$) are shown in Figure 2 for both short-latency (tropical) and long-latency (temperate) strains. For long-latency strains, due to the enforced dormancy period, there is a delay of approximately 100 days, during which a hypnozoite may die, but is highly unlikely to activate; short-latency hypnozoites, in contrast, may activate immediately after they are established in the liver. Upon drug treatment $s_1 = 200$ days after inoculation, all active infections (state A) are modelled to clear (state C) instantaneously, while a hypnozoite in the liver (state H) is modelled to die instantaneously (state D) with probability p_{rad} , leading to jump discontinuities in the state probabilities at time $t = s_1$. Each hypnozoite has two possible end states: death prior to activation (state D), or clearance of the blood-stage infection triggered by activation (state C). The steady-state probability of hypnozoite activation, given by the limit $p_C(t)$ as $t \rightarrow \infty$, is

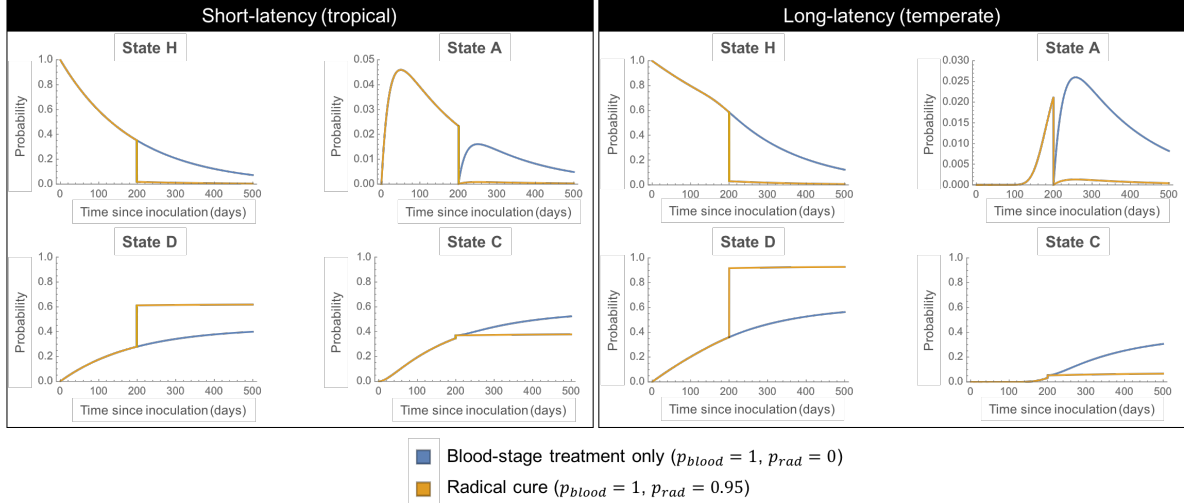


Figure 2: Activation-clearance dynamics, accounting for drug treatment at time $s_1 = 200$ days after inoculation, for both short-latency and long-latency hypnozoites using biologically-plausible parameter values. Baseline activation and clearance rates $\alpha = 1/334 \text{ day}^{-1}$ and $\mu = 1/442 \text{ day}^{-1}$, as well as the rate of progression through successive latency compartments $\delta = 1/5 \text{ day}^{-1}$ and the number of latency compartments $k = 35$ have been obtained from White, Karl, et al. (2014). We further assume a clearance rate $\gamma = 1/20 \text{ day}^{-1}$ for blood-stage infection. We show the case of $p_{\text{blood}} = 1, p_{\text{rad}} = 0$ (blood-stage treatment only) and $p_{\text{blood}} = 1, p_{\text{rad}} = 0.95$ (reasonably effective radical cure).

higher in the absence of radical cure.

3 Hypnozoite and Infection Dynamics in a General Transmission Setting

We will now embed our relapse-clearance model in an epidemiological framework accounting for repeated mosquito inoculation. In previous work, we constructed an infinite server queue, with each departure corresponding to a hypnozoite activation event, to examine the cumulative number of relapses experienced in the interval $(0, t]$ in the absence of treatment, assuming an empty hypnozoite reservoir at time zero (Mehra et al. 2021). Here, we construct an open *network* of infinite server queues (Harrison and Lemoine 1981) to jointly characterise at time t the size of the hypnozoite reservoir; the number of ongoing relapses and primary infections; the number of relapses that have already been cleared; and the number of hypnozoites that have died prior to activation, whilst accounting for drug treatment (Section 3.2). We also extend our previous work to examine the cumulative number of blood-stage infections (that is, both primary infections and relapses) following drug treatment (Section 3.3).

3.1 Epidemiological Framework

We begin by extending the epidemiological framework introduced in Mehra et al. (2021) to account for drug treatment and the dynamics of blood-stage infection. We assume that:

- Infective mosquito bites follow a non-homogenous Poisson process with time-dependent rate $\lambda(t)$ such that the mean number of bites in the interval $(0, t]$, given by $m(t) = \int_0^t \lambda(\tau) d\tau < \infty$ for all $t \geq 0$;
- Each mosquito bite establishes hypnozoites and, with probability p_{prim} , triggers a primary infection (state P), with independent dynamics for each bite;
- In the absence of treatment, blood-stage infections (primary and relapses) are cleared at rate γ (that is, exponentially-distributed with expected duration $1/\gamma$);
- Any ongoing blood-stage infections (primary and relapses) are cleared instantaneously with probability p_{blood} upon drug administration;
- The number of hypnozoites established by each mosquito bite is geometrically-distributed with mean ν , as per White, Karl, et al. (2014); and
- Hypnozoite dynamics are independent and identically distributed (i.i.d.), with probability masses across states $1, \dots, k, NL, A, C, D$ given by
 - Equations (8) to (12) in the absence of drug treatment
 - Equations (23) to (27) given drug treatment is administered time s_1 after inoculation in the liver, where we assume that the drug instantaneously clears relapses (state A to state C) with probability p_{blood} and kills hypnozoites in the liver (states $1, \dots, k, NL$, collectively referred to as state H , to state D) with probability p_{rad} .

3.2 Open Network of Infinite Server Queues

To characterise hypnozoite and infection dynamics in a general transmission setting, we now construct an open network of infinite server queues, denoted $1, \dots, k, NL, A, D, C, P, PC$ (Figure 3). The arrival process for our network is comprised of mosquito bites, which we model as a non-homogeneous Poisson process with rate parameter $\lambda(t)$. Each mosquito bite is associated with a batch arrival (geometrically-distributed, with mean ν) into either queue 1 in the case of long-latency strains ($k > 0$), or queue NL in the case of short-latency strains ($k = 0$), that is, a variable hypnozoite inoculum; and, with probability p_{prim} , a single arrival into queue P , that

is, a primary infection.

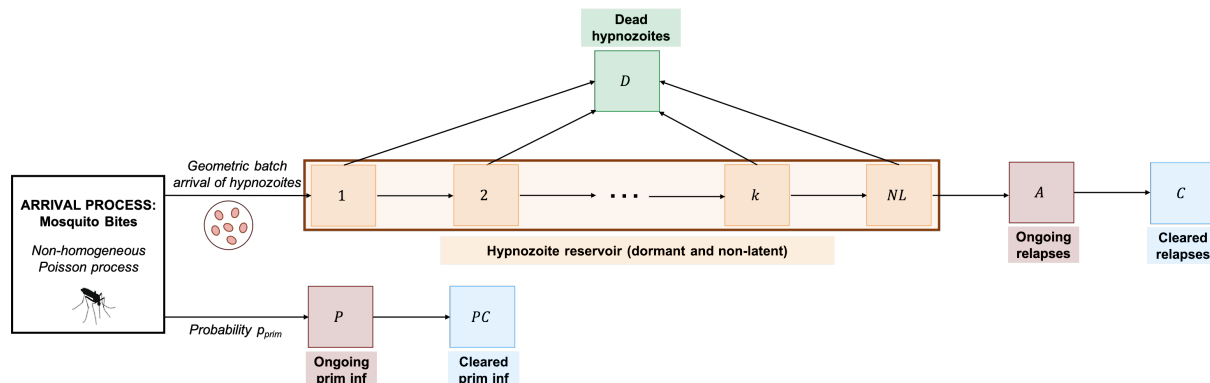


Figure 3: Schematic for open network of infinite server queues.

For $m \in [1, k]$, in the absence of treatment, service times in queue m are exponentially-distributed with rate $(\delta + \mu)$; a departure from queue m may either be routed to queue $(m + 1)$ (that is, the subsequent latency compartment) with probability $\delta/(\delta + \mu)$, or queue D (that is, die due to the death of the host cell) with probability $\mu/(\delta + \mu)$. In contrast, service times in queue NL are exponentially-distributed with parameter $\alpha + \mu$ in the absence of treatment; departures from queue NL (that is, hypnozoites that have been cleared from the liver) are either routed to queue D with probability $\mu/(\alpha + \mu)$, where they remain indefinitely (corresponding to hypnozoites that die prior to activation); or queue A with probability $\alpha/(\alpha + \mu)$ (having activated to trigger a relapse). Upon the administration of drug treatment, with probability p_{rad} , each hypnozoite in queue $1, \dots, k, NL$ is immediately routed to queue D (that is, killed due to radical cure).

Service times in both queues A and P , which correspond to the duration of relapses and primary infections respectively, are exponentially-distributed with rate γ in the absence of treatment. Upon the administration of drug treatment, with probability p_{blood} , each relapse immediately departs queue A , while each primary infection immediately departs queue P . Departures from queues A and P (that is, cleared relapses and primary infections) are routed to queues C and PC respectively, where they remain indefinitely.

For a single hypnozoite that enters either queue 1 in the case of long-latency strains ($k > 0$) or queue NL in the case of short-latency strains ($k = 0$), our network of queues captures precisely those dynamics discussed in Section 2, with the probability of the hypnozoite being present in queue $s \in \{1, \dots, k, NL, A, C, D\}$ at time t after inoculation (that is, arrival into the network)

given by the state probabilities (23) to (27). Upon inoculation, we assume that each hypnozoite and infection behaves independently (Harrison and Lemoine 1981).

Suppose an individual is first exposed to infective mosquito bites at time zero. Let $N_s(t)$ denote the number of hypnozoites/infections at time t in queue $s \in \{1, \dots, k, NL, A, C, D, P\} =: S$. We seek to derive a probability generating function (PGF) for the random vector

$$\mathbf{N}(t) = (N_1(t), N_2(t), \dots, N_k(t), N_{NL}(t), N_A(t), N_C(t), N_D(t), N_P(t), N_{PC}(t)).$$

At time zero, we assume an empty hypnozoite reservoir with no prior infection history, that is,

$$\mathbf{N}(0) = \mathbf{0}.$$

For notational convenience, we introduce a superscript $\mathbf{N}^{t_1}(t)$ to capture the administration of radical cure at time t_1 ; the absence of a superscript indicates a scenario with no drug treatment.

We analyse this network of queues by first considering the case of a single arrival event (mosquito bite). In Section 3.2.1, we examine hypnozoite and infection dynamics for a single mosquito bite in the absence of treatment; we extend this analysis to account for drug treatment in Section 3.2.2. By examining the properties of the non-homogeneous Poisson process governing mosquito bites, we obtain a PGF for $\mathbf{N}(t)$ in Section 3.2.3.

3.2.1 Dynamics for a Single Bite in the Absence of Treatment

Here we consider a single mosquito bite at time τ in the absence of drug treatment. To characterise infection and hypnozoite dynamics arising from the bite, we condition on the size of the hypnozoite inoculum.

We begin by examining hypnozoites and relapses only. Suppose a single hypnozoite is established in the liver (that is, enters the network of queues) at time τ . Then the joint PGF for the number of hypnozoites in each queue $S_h = \{1, \dots, k, NL, A, C, D\}$ at the $t \geq \tau$ follows readily from the state probabilities for a single hypnozoite, for which we have analytic solutions given by Equations (8) to (12)

$$\mathbb{E} \left[\prod_{s \in S_h} z_s^{N_s(t)} \mid 1 \text{ hypnozoite at time } \tau \right] = \sum_{s \in S_h} z_s \cdot p_s(t - \tau).$$

Now, suppose a bite establishing exactly n hypnozoites occurs at time τ , that is, a batch of n hypnozoites enters the queue at time τ . Assuming that hypnozoite dynamics are i.i.d., it follows

that

$$\mathbb{E} \left[\prod_{s \in S_h} z_s^{N_s(t)} \mid n \text{ hypnozoites at time } \tau \right] = \left(\sum_{s \in S_h} z_s \cdot p_s(t - \tau) \right)^n.$$

Given the number of hypnozoites established by each mosquito bite is geometrically-distributed with mean ν , by the law of total expectation,

$$\begin{aligned} \mathbb{E} \left[\prod_{s \in S_h} z_s^{N_s(t)} \mid \text{bite at time } \tau \right] &= \sum_{n=0}^{\infty} \frac{1}{\nu + 1} \left(\frac{\nu}{\nu + 1} \right)^n \cdot \mathbb{E} \left[\prod_{s \in S_h} z_s^{N_s(t)} \mid n \text{ hypnozoites at time } \tau \right] \\ &= \frac{1}{\nu + 1} \sum_{n=0}^{\infty} \left(\sum_{s \in S_h} z_s \cdot p_s(t - \tau) \right)^n \left(\frac{\nu}{1 + \nu} \right)^n \\ &= \frac{1}{1 + \nu \left(1 - \sum_{s \in S_h} z_s \cdot p_s(t - \tau) \right)}, \end{aligned} \quad (28)$$

where the geometric series summation converges in the domain $|z_s| \leq 1$ for all $s \in S_h$.

Recall that each mosquito bite is assumed to trigger a primary infection with probability p_{prim} , with primary infections cleared at rate γ . The joint PGF for the number of ongoing ($N_P(t)$) and cleared ($N_{PC}(t)$) primary infections at time $t \geq \tau$ arising from the bite is therefore

$$\mathbb{E} \left[z_P^{N_P(t)} z_{PC}^{N_{PC}(t)} \mid \text{bite at time } \tau \right] = \underbrace{(1 - p_{\text{prim}})}_{\text{no prim inf due to bite}} + \underbrace{p_{\text{prim}} e^{-\gamma(t-\tau)}}_{\text{ongoing prim inf at time } t} z_P + \underbrace{p_{\text{prim}} (1 - e^{-\gamma(t-\tau)})}_{\text{prim inf cleared by time } t} z_{PC}. \quad (29)$$

Given primary infection dynamics are independent of hypnozoite and relapse dynamics, it follows from Equation (28) (the joint PGF for $(N_1(t), N_2(t), \dots, N_k(t), N_{NL}(t), N_A(t), N_C(t), N_D(t))$) and Equation (29) (the joint PGF for $(N_P(t), N_{PC}(t))$) that

$$\begin{aligned} \mathbb{E} \left[\prod_{s \in S} z_s^{N_s(t)} \mid \text{bite at time } \tau \right] &= \mathbb{E} \left[\prod_{s \in S_h} z_s^{N_s(t)} \mid \text{bite at time } \tau \right] \cdot \mathbb{E} \left[z_P^{N_P(t)} z_{PC}^{N_{PC}(t)} \mid \text{bite at time } \tau \right] \\ &= \frac{p_{\text{prim}} e^{-\gamma(t-\tau)} z_P + p_{\text{prim}} (1 - e^{-\gamma(t-\tau)}) z_{PC} + (1 - p_{\text{prim}})}{1 + \nu \left(1 - \sum_{s \in S_h} z_s \cdot p_s(t - \tau) \right)}. \end{aligned} \quad (30)$$

We note that Equation (30) holds in the domain $|z_s| \leq 1$ for each $s \in S$.

Given a single mosquito bite at time $\tau \leq t$, Equation (30) characterises the joint PGF for the number of hypnozoites/infections in each queue $S \in \{1, \dots, k, NL, A, C, D, P, PC\}$ at time t in the absence of treatment.

3.2.2 Dynamics for a Single Bite Under Drug Treatment

Now, suppose that drug treatment is administered at time t_1 , instantaneously killing each hypnozoite in the liver with probability p_{rad} and clearing each ongoing blood-stage infection (primary or relapse) with probability p_{blood} . Here, we consider the case $t \geq t_1$.

As in Section 3.2.1, we begin by considering a single hypnozoite that is established in the liver at time τ to obtain

$$\mathbb{E} \left[\prod_{s \in S_h} z_s^{N_s^{t_1}(t)} \mid 1 \text{ hypnozoite at time } \tau \right] = \sum_{s \in S_h} z_s \cdot p_s^r(t - \tau, t_1 - \tau),$$

where the probability $p_s^r(t - \tau, t_1 - \tau)$ of a hypnozoite being in queue $s \in S_h = \{1, \dots, k, NL, A, C, D\}$ at time $t \geq t_1$, accounting for drug treatment at time t_1 , is given by Equations (23) to (27).

Assuming that hypnozoite dynamics are i.i.d. and hypnozoite inocula are geometrically distributed with mean ν , using similar reasoning to Section 3.2.1, it follows that

$$\mathbb{E} \left[\prod_{s \in S_h} z_s^{N_s^{t_1}(t)} \mid \text{bite at time } \tau \right] = \frac{1}{1 + \nu \left(1 - \sum_{s \in S_h} z_s \cdot p_s^r(t - \tau, t_1 - \tau) \right)}, \quad (31)$$

where the RHS is well-defined in the domain $|z_s| \leq 1$ for each $s \in S_h$. Equation (31) characterises hypnozoite and relapse dynamics for a single bite following drug treatment. We next account for primary infections, which occur with probability p_{prim} for each mosquito bite. In the case of a bite that occurs after drug treatment, that is, $\tau \geq t_1$, primary infections are unaffected by drug treatment, hence

$$\mathbb{E} \left[z_P^{N_P^{t_1}(t)} z_{PC}^{N_{PC}^{t_1}(t)} \mid \text{bite at time } \tau \geq t_1 \right] = (1 - p_{\text{prim}}) + p_{\text{prim}} e^{-\gamma(t-\tau)} z_P + p_{\text{prim}} (1 - e^{-\gamma(t-\tau)}) z_{PC}$$

as per Equation (29). For bites prior to drug treatment, that is $\tau < t_1$, the joint PGF for the number of ongoing ($N_P^{t_1}(t)$) and cleared ($N_{PC}^{t_1}(t)$) primary infections at time $t \geq t_1$ is given by

$$\begin{aligned} \mathbb{E} \left[z_P^{N_P^{t_1}(t)} z_{PC}^{N_{PC}^{t_1}(t)} \mid \text{bite at time } \tau < t_1 \right] &= \underbrace{(1 - p_{\text{prim}})}_{\text{no prim inf due to bite}} + \underbrace{p_{\text{prim}}(1 - p_{\text{blood}})e^{-\gamma(t-\tau)}}_{\text{ongoing prim inf at time } t \geq t_1 \text{ that survives drug at time } t_1} z_P + \\ &\left(\underbrace{p_{\text{prim}} p_{\text{blood}} e^{-\gamma(t_1-\tau)}}_{\text{prim inf cleared due to drug at time } t_1} + \underbrace{p_{\text{prim}}(1 - p_{\text{blood}})e^{-\gamma(t_1-\tau)}[1 - e^{-\gamma(t-t_1)}]}_{\text{prim inf that survives drug at time } t_1 \text{ cleared naturally by time } t} + \underbrace{p_{\text{prim}}(1 - e^{-\gamma(t_1-\tau)})}_{\text{prim inf cleared naturally before treatment at time } t_1} \right) z_{PC}. \end{aligned} \quad (32)$$

Assuming hypnozoite dynamics are independent to primary infections, for $t \geq t_1$, it follows from Equation (31) (the joint PGF for $(N_1^{t_1}(t), N_2^{t_1}(t), \dots, N_k^{t_1}(t), N_{NL}^{t_1}(t), N_A^{t_1}(t), N_C^{t_1}(t), N_D^{t_1}(t))$) and

Equations (29) and (32) (the joint PGF for $(N_P^{t_1}(t), N_{PC}^{t_1}(t))$ in the cases $\tau \geq t_1$ and $\tau < t_1$ respectively) that

$$\begin{aligned} \mathbb{E} \left[\prod_{s \in S} z_s^{N_s^{t_1}(t)} \mid \text{bite at time } \tau \right] &= \mathbb{E} \left[\prod_{s \in S_h} z_s^{N_s^{t_1}(t)} \mid \text{bite at time } \tau \right] \cdot \mathbb{E} \left[z_P^{N_P^{t_1}(t)} z_{PC}^{N_{PC}^{t_1}(t)} \mid \text{bite at time } \tau \right] \\ &= \begin{cases} \frac{1 - p_{\text{prim}} + p_{\text{prim}} e^{-\gamma(t-\tau)} z_P + p_{\text{prim}} (1 - e^{-\gamma(t-\tau)}) z_{PC}}{1 + \nu \left(1 - \sum_{s \in S_h} z_s \cdot p_s(t-\tau) \right)} & \text{if } \tau \geq t_1 \\ \frac{1 - p_{\text{prim}} + p_{\text{prim}} (1 - p_{\text{blood}}) e^{-\gamma(t-\tau)} z_P + p_{\text{prim}} (1 - (1 - p_{\text{blood}}) e^{-\gamma(t-\tau)}) z_{PC}}{1 + \nu \left(1 - \sum_{s \in S_h} z_s \cdot p_s^*(t-\tau, t_1-\tau) \right)} & \text{if } \tau < t_1 \end{cases}. \end{aligned} \quad (33)$$

where $S_h = \{1, 2, \dots, k, NL, A, C, D\}$ denotes the state space for a single hypnozoite. We note that Equation (33) holds in the domain $|z_s| \leq 1$ for each $s \in S$.

For a single a mosquito bite at time $\tau \leq t$, the joint PGF in Equation (33) characterises the number of hypnozoites/infections in each queue $S \in \{1, \dots, k, NL, A, C, D, P, PC\}$ at time $t \geq t_1$, given the administration of a drug at time t_1 . An illustrative sample path, generated using direct stochastic simulation (using the Doob-Gillespie algorithm) of short-latency hypnozoite dynamics, is shown in Figure 4. At time $t = 0$, an infective mosquito bite establishes 14 hypnozoites in the host liver, and triggers a primary infection; radical cure is administered $t = 100$ days following the mosquito bite, as indicated by the vertical red line. Prior to $t = 100$ days, the number of hypnozoites in the liver (state H) decreases over time as hypnozoites either activate to cause relapses (state A) or die prior to activation (state D) at constant rates. Hypnozoite activation events in quick succession lead to overlapping relapses for a brief period of time, with all relapses eventually cleared (state C). Upon the administration of radical cure (vertical red line), seven of the eight remaining hypnozoites within the liver are instantaneously killed. The final hypnozoite then dies, prior to activation, approximately 160 days after the mosquito bite.

3.2.3 Mosquito Inoculation

We now consider the non-homogeneous Poisson process (of rate $\lambda(t)$) governing mosquito bites. To characterise the PGF for $\mathbf{N}(t)$ as a function of hypnozoite and infection dynamics for a single mosquito bite (as examined in Sections 3.2.1 and 3.2.2), we first condition on the number of mosquito bites in a given interval, and then the bite times themselves, following the procedure detailed in Mehra et al. (2021) and based on Parzen (1999).

Let $M(t)$ denote the number of infective mosquito bites in the interval $(0, t]$, with respective

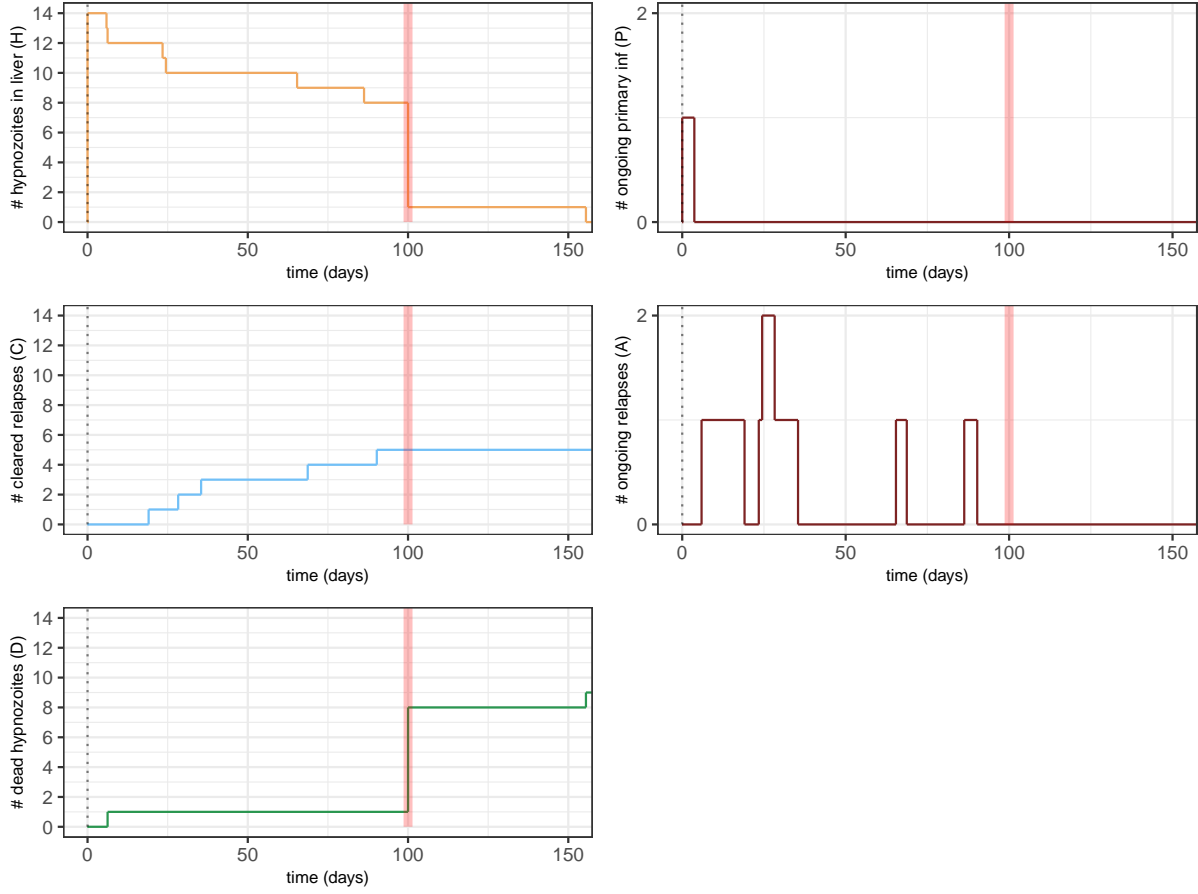


Figure 4: Simulated sample path for a single mosquito bite, assuming short-latency (tropical) strains. At time $t = 0$, an infective mosquito bite triggers a primary infection and establishes 14 hypnozoites in the host liver. We account for the administration of radical cure ($p_{\text{rad}} = 0.95$, $p_{\text{blood}} = 1$) at time $t = 100$ days following the bite. Hypnozoite activation and death rates, $\alpha = 1/334 \text{ day}^{-1}$ and $\mu = 1/442 \text{ day}^{-1}$, are based on estimates by White, Karl, et al. (2014). The clearance rate for blood-stage infections has been set to $\gamma = 1/20 \text{ day}^{-1}$.

bite times T_i , $i \in \{1, \dots, M(t)\}$. Applying the law of total expectation and recalling that $M(t) \sim \text{Poisson}(m(t))$, where $m(t) = \int_0^t \lambda(\tau) d\tau$ denotes the mean number of bites in the interval $(0, t]$, we have

$$\mathbb{E} \left[\prod_{s \in S} z_s^{N_s(t)} \right] = \sum_{m=0}^{\infty} \frac{m(t)^m e^{-m(t)}}{m!} \mathbb{E} \left[\prod_{s \in S} z_s^{N_s(t)} | M(t) = m \right]. \quad (34)$$

where $S = \{1, \dots, k, NL, A, C, D, P, PC\}$ denotes the set of queues in the network.

Now, suppose $M(t) = m$, that is, precisely m bites occur in the interval $(0, t]$. Assuming that hypnozoite and infection dynamics arising from each mosquito bite are independent, we have

$$\mathbb{E} \left[\prod_{s \in S} z_s^{N_s(t)} | M(t) = m, T_1 = \tau_1, \dots, T_m = \tau_m \right] = \prod_{j=1}^m \mathbb{E} \left[\prod_{s \in S} z_s^{N_s(t)} | \text{bite at time } \tau_j \right]. \quad (35)$$

As per Lewis (1967), the bite times T_1, \dots, T_m have a conditional distribution equivalent to m i.i.d. random variables with density

$$f(\tau) = \frac{\lambda(\tau)}{m(t)} \mathbb{1}\{\tau \in [0, t]\},$$

and thus have joint density

$$f_{T_1, \dots, T_m}(\tau_1, \dots, \tau_m) = \prod_{j=1}^m f(\tau_j) = \frac{1}{m(t)^m} \prod_{j=1}^m \lambda(\tau_j) \mathbb{1}(\tau_j \in (0, t]). \quad (36)$$

By integrating the conditional expectation given by Equation (35) over the joint density given by Equation (36), we obtain

$$\begin{aligned} & \mathbb{E} \left[\prod_{s \in S} z_s^{N_s(t)} | M(t) = m \right] \\ &= \int_0^\infty d\tau_1 \cdots \int_0^\infty d\tau_m \mathbb{E} \left[\prod_{s \in S} z_s^{N_s(t)} | M(t) = m, T_1 = \tau_1, \dots, T_m = \tau_m \right] f_{T_1, \dots, T_m}(\tau_1, \dots, \tau_m) \\ &= \frac{1}{m(t)^m} \int_0^t d\tau_1 \cdots \int_0^t d\tau_m \prod_{j=1}^m \left\{ \lambda(\tau_j) \mathbb{E} \left[\prod_{s \in S} z_s^{N_s(t)} | \text{bite at time } \tau_j \right] \right\} \\ &= \left(\frac{1}{m(t)} \int_0^t \lambda(\tau) \mathbb{E} \left[\prod_{s \in S} z_s^{N_s(t)} | \text{bite at time } \tau \right] d\tau \right)^m. \end{aligned} \quad (37)$$

Substituting Equation (37) into Equation (34) yields the joint PGF for $\mathbf{N}(t)$ in a general trans-

mission setting as a function of the PGF for a single mosquito bite:

$$\begin{aligned}\mathbb{E} \left[\prod_{s \in S} z_s^{N_s(t)} \right] &= e^{-m(t)} \sum_{m=0}^{\infty} \frac{m(t)^m}{m!} \left[\frac{1}{m(t)} \int_0^t \lambda(\tau) \mathbb{E} \left[\prod_{s \in S} z_s^{N_s(t)} \mid \text{bite at time } \tau \right] d\tau \right]^m \\ &= \exp \left\{ -m(t) + \int_0^t \lambda(\tau) \mathbb{E} \left[\prod_{s \in S} z_s^{N_s(t)} \mid \text{bite at time } \tau \right] d\tau \right\},\end{aligned}\quad (38)$$

where the RHS has been simplified using the Taylor series expansion of the exponential function.

To capture hypnozoite and infection dynamics in the absence of drug treatment, we substitute Equation (30) into Equation (38) to yield the joint PGF for $\mathbf{N}(t)$,

$$\begin{aligned}G(t, z_1, \dots, z_k, z_{NL}, z_A, z_D, z_C, z_P, z_{PC}) &:= \mathbb{E} \left[\prod_{s \in S} z_s^{N_s(t)} \right] \\ &= \exp \left\{ -m(t) + \int_0^t \lambda(\tau) \frac{1 - p_{\text{prim}} + p_{\text{prim}} e^{-\gamma(t-\tau)} z_P + p_{\text{prim}} (1 - e^{-\gamma(t-\tau)}) z_{PC}}{1 + \nu \left(1 - \sum_{s \in S_h} z_s \cdot p_s(t-\tau) \right)} d\tau \right\}.\end{aligned}\quad (39)$$

In the case where drug treatment is administered at time t_1 , we obtain the joint PGF for $\mathbf{N}^{t_1}(t)$ by substituting Equation (33) in Equation (37):

$$\begin{aligned}G^{t_1}(t, z_1, \dots, z_k, z_{NL}, z_A, z_D, z_C, z_P, z_{PC}) &:= \mathbb{E} \left[\prod_{s \in S} z_s^{N_s^{t_1}(t)} \right] \\ &= \exp \left\{ -m(t) + \int_{t_1}^t \lambda(\tau) \frac{1 - p_{\text{prim}} + p_{\text{prim}} e^{-\gamma(t-\tau)} z_P + p_{\text{prim}} (1 - e^{-\gamma(t-\tau)}) z_{PC}}{1 + \nu \left(1 - \sum_{s \in S_h} z_s \cdot p_s(t-\tau) \right)} d\tau + \right. \\ &\quad \left. \int_0^{t_1} \lambda(\tau) \frac{1 - p_{\text{prim}} + p_{\text{prim}} (1 - p_{\text{blood}}) e^{-\gamma(t-\tau)} z_P + p_{\text{prim}} (1 - (1 - p_{\text{blood}}) e^{-\gamma(t-\tau)}) z_{PC}}{1 + \nu \left(1 - \sum_{s \in S_h} z_s \cdot p_s^r(t-\tau, t_1-\tau) \right)} d\tau \right\}.\end{aligned}\quad (40)$$

Both Equations (39) and (40) are well-defined in the domain $|z_s| \leq 1$ for each $s \in S$. Here, we recall that

- Mosquito bites follow a non-homogeneous Poisson process with rate $\lambda(t)$, with the mean number of bites in the interval $(0, t]$ given by $m(t) = \int_0^t \lambda(\tau) d\tau$;
- Each bite triggers a primary infection with probability p_{prim} and establishes geometrically-distributed hypnozoite inocula with mean ν ;
- Blood-stage infections (primary or relapse) are cleared at rate γ at baseline, but are cleared instantaneously with probability p_{blood} upon treatment at time t_1 ;

- State probabilities for a single hypnozoite, with state space $S_h = \{1, \dots, k, NL, A, C, D\}$ are given by Equations (8) to (12) in the absence of treatment (p_s) and Equations (23) to (27) following drug treatment at time t_1 (p_s^r), with the latter state probabilities accounting for each hypnozoite in the liver (states $1, \dots, k, NL$) being killed instantaneously (state D) with probability p_{rad} upon treatment.

An illustrative sample path of infection dynamics for an individual in a constant transmission setting is shown in Figure 5, assuming short-latency (tropical) strains. Activation-clearance dynamics for each hypnozoite have been simulated using direct stochastic simulation (using the Doob-Gillespie algorithm). At time $t = 0$, we assume that the individual has both an empty hypnozoite reservoir and no ongoing infections. In this simulation, an individual receives four infective bites (as indicated with dashed vertical lines) over a two-year period, with two bites triggering primary infections (state P). The hypnozoite reservoir (state H) fluctuates in size as hypnozoites are replenished through infective mosquito bites, but removed from the liver, either due to activation, thereby triggering relapses (state A), or death (state D). Hypnozoite activation events in quick succession give rise to overlapping relapses (that is, multiple infections). Radical cure, administered after the hypnozoite reservoir has been allowed to accumulate for $t = 365$ days (indicated with a vertical red line), kills the entire hypnozoite reservoir and instantaneously clears an ongoing relapse.

3.3 Recurrences Following Drug Treatment

In Sections 3.2.1 and 3.2.2, we examined the dynamics of the hypnozoite reservoir in an interval $(0, t]$, where time zero marks the time of first exposure in the epidemiological setting. Here, under the same epidemiological framework, we instead consider the cumulative number of recurrences in the interval $(t_1, t_2]$ following drug treatment at time t_1 . Denoting

$$I_C(t) = N_A(t) + N_C(t) + N_P(t) + N_{PC}(t),$$

we seek to derive a PGF for the quantity $I_C(t_2) - I_C(t_1)$. The number of recurrences following drug treatment can provide insight into the impact of drug treatment on the infection burden. Since the random variables $I_C(t_2) - I_C(t_1)$ and $I_C(t_1)$ are not independent, we cannot characterise the quantity $I_C(t_2) - I_C(t_1)$ directly from the results in Section 3.2.

Similarly to Mehra et al. (2021), we now construct an infinite server queue, such that the departure process counts the cumulative number of recurrences over time (Figure 6). Noting that the departure process of an infinite server queue constitutes a shot noise process (Holman,

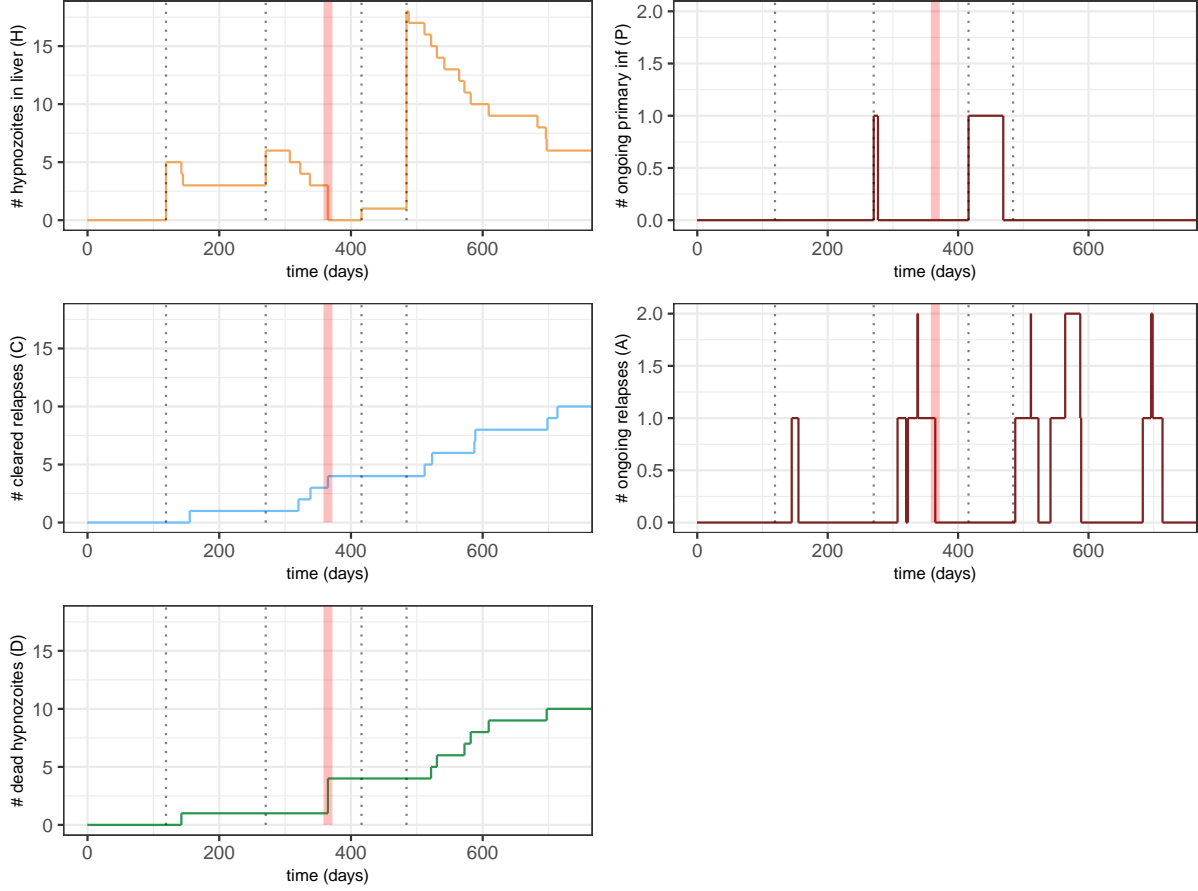


Figure 5: Simulated infection and hypnozoite dynamics for an individual in a constant transmission setting, assuming short-latency (tropical) strains. At time $t = 0$, we assume an empty hypnozoite reservoir, with no ongoing infections. Radical cure ($p_{\text{rad}} = 0.95$, $p_{\text{blood}} = 1$) is administered after the hypnozoite reservoir has accumulated for $t = 365$ days. In this simulation, an individual is bitten four times over a two year period, as indicated with dashed vertical lines. Mosquito bites have been modelled to follow a Poisson process with constant rate $\lambda = 3/365 \text{ day}^{-1}$, with each bite establishing an average of $\nu = 9$ hypnozoites in the liver (as per estimates from White, Karl, et al. (2014)) and triggering a relapse with probability $p_{\text{prim}} = 0.5$. Hypnozoite activation and death rates, $\alpha = 1/334 \text{ day}^{-1}$ and $\mu = 1/442 \text{ day}^{-1}$, are based on estimates by White, Karl, et al. (2014). The clearance rate for blood-stage infections has been set to $\gamma = 1/20 \text{ day}^{-1}$.

Chaudhry, and Kashyap 1983), the total number of recurrences in the interval $[0, t_2]$, $t_2 \geq t_1$ can be written

$$I_C(t_2) = \underbrace{\sum_{m=1}^{N(t_1)} (M_m^r(t_2 - \tau_m) + V_m)}_{\# \text{ recurrences from bites in } (0, t_1]} + \underbrace{\sum_{m=N(t_1)+1}^{N(t_2)} (M_m(t_2 - \tau_m) + V_m)}_{\# \text{ recurrences from bites in } (t_1, t_2]}$$

where

- $N(t) \sim \text{Poisson}(m(t))$ denotes the number of mosquito bites in the interval $[0, t]$, with $\tau_1, \dots, \tau_{N(t)}$ denoting the respective bite times;
- $M_m^r(t_2 - \tau_m)$ are independent random variables, representing the number of hypnozoite activation events at time t_2 arising from a bite that occurred at time $\tau_m < t_1$ whilst accounting for drug treatment at time t_1
- $M_m(t_2 - \tau_m)$ are independent random variables representing the number of hypnozoite activation events at time t_2 arising from a bite that occurred at time $\tau_m > t_1$ and are thus unaffected by drug treatment; and
- $V_m \stackrel{iid}{\sim} \text{Bernoulli}(p_{\text{prim}})$ represent primary infections, which occur independently with probability p_{prim} as a result of each mosquito bite.

We seek to characterise the number of recurrences in the interval $(t_1, t_2]$, that is,

$$\begin{aligned} I_C(t_2) - I_C(t_1) &= \underbrace{\sum_{m=0}^{N(t_1)} (M_m^r(t_2 - \tau_m) - M_m^r(t_1 - \tau_m))}_{\# \text{ recurrences initiated in } (t_1, t_2] \text{ from bites in } (0, t_1]} + \underbrace{\sum_{m=N(t_1)+1}^{N(t_2)} (M_m(t_2 - \tau_m) + V_m)}_{\# \text{ recurrences initiated in } (t_1, t_2] \text{ from bites in } (t_1, t_2]} \\ &=: I_{C_1}(t_1, t_2) + I_{C_2}(t_1, t_2). \end{aligned} \quad (41)$$

Only hypnozoites and infections established before time t_1 are affected by drug treatment; for all bites following drug treatment, we revert to the scenario detailed in Section 3.2.1, which does not consider drug treatment. As such, setting $t_1 = 0$ in Equation (41) yields the cumulative number of infections in the interval $(0, t_2]$, where zero represents the time since an individual is first exposed to infective mosquito bites, in the absence of treatment.

By the independent increment property of the Poisson process, the number of bites in the disjoint

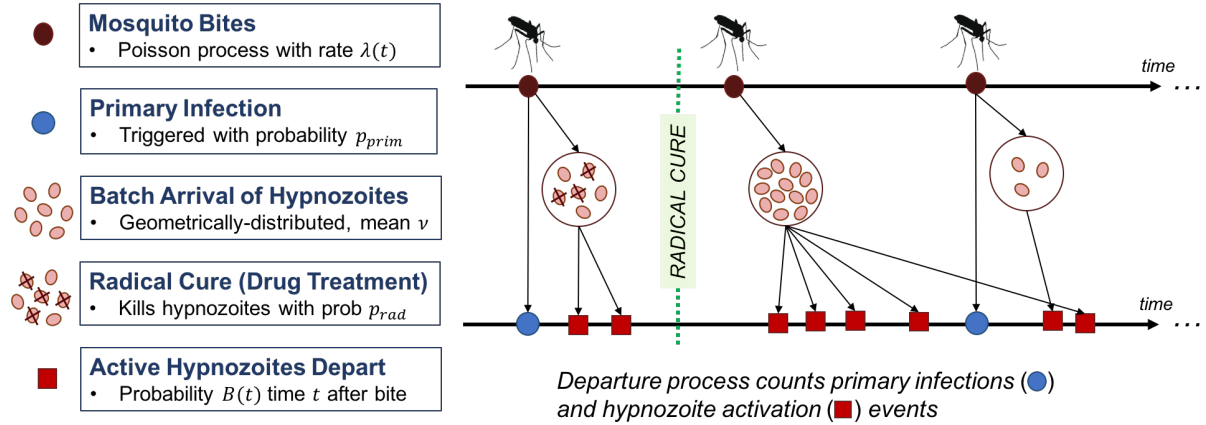


Figure 6: Schematic for model of *P. vivax* recurrences. To capture recurrences due to both reinfection and hypnozoite activation, we construct an infinite server queue. Arrivals, which represent mosquito bites, occur according to a non-homogeneous Poisson process with time-dependent rate $\lambda(t)$. Each mosquito bite triggers a primary infection with probability p_{prim} , and also leads to the establishment of hypnozoites in the liver. The hypnozoite inoculum associated with each bite is assumed geometrically-distributed with mean ν . The service time of each hypnozoite is i.i.d. with distribution $B(t) = p_A(t) + p_C(t)$ (Equation (43), which describes the probability that a hypnozoite has activated time t after inoculation, noting that not every hypnozoite necessarily activates (that is, it is not guaranteed that $\lim_{t \rightarrow \infty} B(t) = 1$). Under this formulation, only active hypnozoites and primary infections depart the queue. The departure process counts the cumulative number of recurrences over time. To model the effects of radical cure, we assume that any hypnozoite established before drug treatment is killed instantaneously with probability p_{rad} upon treatment.

intervals

$$\begin{aligned} (0, t_1] : N(t_1) &\sim \text{Poisson}(m(t_1)) \\ (t_1, t_2] : N(t_2) - N(t_1) &\sim \text{Poisson}(m(t_2) - m(t_1)) \end{aligned}$$

are independent random variables. The bite times in the intervals $(0, t_1]$ and $(t_1, t_2]$ are also independent. Given the dynamics of each hypnozoite and primary infection are independent, it follows that $I_{C_1}(t_1, t_2)$ and $I_{C_2}(t_1, t_2)$, the number of recurrences triggered in $(t_1, t_2]$ by bites in the intervals $(0, t_1]$ and $(t_1, t_2]$ respectively, are independent. Thus, from Equation (41), the PGF for $I_C(t_2) - I_C(t_1)$ is given by the product

$$\mathbb{E} [z^{I_C(t_2) - I_C(t_1)}] = \mathbb{E} [z^{I_{C_1}(t_1, t_2)}] \mathbb{E} [z^{I_{C_2}(t_1, t_2)}]. \quad (42)$$

We therefore proceed by considering mosquito bites in the intervals $(0, t_1]$ and $(t_1, t_2]$ separately.

We begin by analysing recurrences arising from a single mosquito bite at time $\tau_m \in (t_1, t_2]$, that is, the random variable $(M_m(t_2 - \tau_m) + V_m)$. Hypnozoites and infections triggered by this bite will *not* be affected by drug treatment.

Suppose a single hypnozoite is established in the liver at time $\tau_m \in (t_1, t_2]$. For notational convenience, we denote the probability this hypnozoite will activate in the interval $(\tau_m, t_2]$ by $B(t_2 - \tau_m)$, where

$$\begin{aligned} B(t) &= p_A(t) + p_C(t) \\ &= \frac{\alpha \delta^k}{(\delta - \alpha)^k} \left[\frac{e^{-(\mu + \delta)t}}{\mu + \delta} \left\{ \sum_{j=0}^{k-1} \left(\frac{\delta - \alpha}{\mu + \delta} \right)^j \sum_{i=0}^j \frac{t^i}{i!} (\mu + \delta)^i \right\} - \frac{e^{-(\mu + \alpha)t}}{\mu + \alpha} \right] + \frac{\alpha}{\alpha + \mu} \left(\frac{\delta}{\delta + \mu} \right)^k \end{aligned} \quad (43)$$

using Equations (10) and (11).

Now, suppose a bite at time $\tau_m \in (t_1, t_2]$ establishes precisely $Q = q$ hypnozoites in the liver. As per Mehra et al. (2021), since each hypnozoite activates in the interval $(\tau, t_2]$ independently with probability $B(t_2 - \tau)$, the number of hypnozoite activation events by time t_2 , $M_m^r(t_2 - \tau)$, has conditional distribution

$$M_m(t_2 - \tau) \sim \text{Binomial}(q, B(t_2 - \tau_m)),$$

and thus conditional PGF

$$\mathbb{E} [z^{M_m(t_2 - \tau)} | Q = q] = (1 + B(t_2 - \tau_m)(z - 1))^q. \quad (44)$$

By the law of total expectation, noting that the size of the hypnozoite inoculum Q is geometrically-distributed with mean ν , it follows that $M_m(t_2 - \tau_m)$ has PGF

$$\mathbb{E} [z^{M_m(t_2 - \tau_m)}] = \sum_{q=0}^{\infty} \frac{1}{\nu + 1} \left(\frac{\nu}{\nu + 1} \right)^q \mathbb{E} [z^{M_m(t_2 - \tau)} | Q = q] = \frac{1}{1 - \nu B(t_2 - \tau_m)(z - 1)} \quad (45)$$

where we have substituted Equation (44) and applied the geometric series summation. We note that Equation (45) holds in the domain $|z| \leq 1$.

Assuming that dynamics of each relapse and primary infection are independent, $M_m(t_2 - \tau_m)$ and V_m are independent random variables. Hence, the PGF for $(M_m(t_2 - \tau_m) + V_m)$, the total number of recurrences in the interval $[\tau_m, t_2)$ arising from a bite at time τ_m , is given by the product

$$\mathbb{E} [z^{M_m(t_2 - \tau_m) + V_m}] = \mathbb{E} [z^{M_m(t_2 - \tau_m)}] \mathbb{E} [z^{V_m}] = \frac{1 - p_{\text{prim}} + z p_{\text{prim}}}{1 - \nu B(t_2 - \tau_m)(z - 1)} \quad (46)$$

where we have noted that $V_m \sim \text{Bernoulli}(p_{\text{prim}})$ and substituted Equation (45).

Now, consider a mosquito bite that occurs at time $\tau_m \in (0, t_1]$, that is, prior to drug treatment. Any hypnozoites or infections arising from this bite may be affected by drug treatment. Here, we consider the random variable $(M^r(t_2 - \tau_m) - M^r(t_1 - \tau_m))$, which describes the number of relapses triggered by the bite in the interval $(t_1, t_2]$.

As before, we begin by examining the case of a single hypnozoite established in the liver at time $\tau_m \in (0, t_1]$, which will activate in the interval (t_1, t_2) with probability

$$\begin{aligned} p_A^r(t_2 - \tau_m, t_1 - \tau_m) + p_C^r(t_2 - \tau_m, t_1 - \tau_m) - p_A^r(t_1 - \tau_m, t_1 - \tau_m) + p_C^r(t_1 - \tau_m, t_1 - \tau_m) \\ = (1 - p_{\text{rad}})(B(t_2 - \tau) - B(t_1 - \tau)), \end{aligned}$$

where $B(t)$ is given by Equation (43).

Suppose that a bite at time $\tau_m \in (0, t_1]$ establishes $Q = q$ hypnozoites. Under the assumption that hypnozoite dynamics are i.i.d., the number of relapses $(M^r(t_2 - \tau_m) - M^r(t_1 - \tau_m))$ triggered in the interval (t_1, t_2) has conditional distribution

$$M_m^r(t_2 - \tau_m) - M_m^r(t_1 - \tau_m) \sim \text{Binomial}(q, (1 - p_{\text{rad}})(B(t_2 - \tau_m) - B(t_1 - \tau_m))).$$

Using similar reasoning to Equations (44) and (45) and applying the law of total expectation to account for a geometrically-distributed hypnozoite inoculum Q , it follows that the random

variable $M^r(t_2 - \tau_m) - M_m^r(t_1 - \tau_m)$ has PGF

$$\mathbb{E} \left[z^{M_m^r(t_2 - \tau_m) - M_m^r(t_1 - \tau_m)} \right] = \frac{1}{1 - \nu(1 - p_{\text{rad}})(B(t_2 - \tau) - B(t_1 - \tau))(z - 1)}, \quad (47)$$

which likewise holds in the domain $|z| \leq 1$.

Equation (47) characterises the number of recurrences arising from a single bite at time $\tau_m \in [0, t_1]$ initiated in the interval (t_1, t_2) , while Equation (45) characterises the number of recurrences arising from a single bite at time $\tau_m \in [t_1, t_2]$ initiated in the interval (τ_m, t_2) .

Next, we examine the distribution of bite times. Given $N(t_2) - N(t') = n$, from Lewis (1967), the conditional distribution of bite times in the interval $[t', t_2)$ is equivalent to n i.i.d. random variables with density

$$f_1(\tau) = \frac{\lambda(\tau)}{m(t_2) - m(t')} \mathbb{1}\{\tau \in [t', t_2)\}.$$

Hence, following a similar procedure to Section 3.2.3, whereby we first condition on the number of bites in the interval, then the distribution of bite times, we have

$$\mathbb{E} \left[z^{I_{C_1}(t_1, t_2)} \right] = \exp \left\{ -m(t_1) + \int_0^{t_1} \lambda(\tau) \mathbb{E} \left[z^{M_m^r(t_2 - \tau) - M_m^r(t_1 - \tau)} \right] d\tau \right\} \quad (48)$$

$$\mathbb{E} \left[z^{I_{C_2}(t_1, t_2)} \right] = \exp \left\{ -(m(t_2) - m(t_1)) + \int_{t_1}^{t_2} \lambda(\tau) \mathbb{E} \left[z^{M_m(t_2 - \tau) + V_m} \right] d\tau \right\}. \quad (49)$$

From Equation (42), since $I_{C_1}(t_1, t_2)$ and $I_{C_2}(t_1, t_2)$ are independent, it follows that

$$\mathbb{E} \left[z^{I_C(t_2) - I_C(t_1)} \right] = \exp \left\{ -m(t_2) + \int_0^{t_1} \lambda(\tau) \mathbb{E} \left[z^{M_m^r(t_2 - \tau) - M_m^r(t_1 - \tau)} \right] d\tau + \right. \quad (50)$$

$$\left. \int_{t_1}^{t_2} \lambda(\tau) \mathbb{E} \left[z^{M_m(t_2 - \tau) + V_m} \right] d\tau \right\}, \quad (51)$$

where we have substituted Equations (48) and (49).

Substituting Equations (46) and (47) into Equation (51) yields the PGF of $I_C(t_2) - I_C(t_1)$:

$$\mathbb{E} \left[z^{I_C(t_2) - I_C(t_1)} \right] = \exp \left\{ -m(t_2) + \int_0^{t_1} \frac{\lambda(\tau)}{1 - \nu(1 - p_{\text{rad}})(B(t_2 - \tau) - B(t_1 - \tau))(z - 1)} d\tau + \int_{t_1}^{t_2} \frac{\lambda(\tau)(1 - p_{\text{prim}} + zp_{\text{prim}})}{1 - \nu B(t_2 - \tau)(z - 1)} d\tau \right\}, \quad (52)$$

which holds in the domain $|z| \leq 1$ and gives us the number of recurrences initiated in the interval $(t_1, t_2]$ following drug treatment at time t_1 , where

- $\lambda(\tau)$ is the infective mosquito bite rate, with the mean number of bites in the interval $(0, t]$ denoted by $m(t) = \int_0^t \lambda(\tau) d\tau$;
- Hypnozoite inocula for each bite are geometrically distributed with mean ν ;
- Each bite triggers a primary infection with probability p_{prim} ;
- $B(t')$ denotes the probability that a hypnozoite has activated time t' after inoculation in the absence of treatment (Equation (43)); and
- Each hypnozoite is killed instantaneously with probability p_{rad} upon administration of radical cure at time t_1 .

4 Quantities of Epidemiological Significance

Using the PGFs derived in Section 3 (Equations (39), (40) and (52)), we can obtain several quantities of epidemiological significance pertaining to the relapse burden and the longer-term impacts of radical cure on the infection burden. Here, we consider an individual who is first exposed to infective mosquito bites at time zero, and is administered radical cure at time t_1 .

4.1 Size of Hypnozoite Reservoir

The risk of relapse for an individual is governed by the size of the hypnozoite reservoir. For short-latency strains, all hypnozoites in the liver (state H) may activate. For long-latency strains, in contrast, the hypnozoite reservoir is comprised of both dormant hypnozoites (states $1, \dots, k$) that can die, but are unable to activate; and non-latent hypnozoites (state NL) that have emerged from dormancy and may now activate. Here, we consider the total number of hypnozoites (state H) in the liver at time t , that is,

$$N_H(t) = N_{NL}(t) + \sum_{m=1}^k N_m(t).$$

The PGF for $N_H(t)$ follows from the joint PGFs for $\mathbf{N}(t)$ (denoted by G in Equation (39), capturing hypnozoite dynamics in the absence of treatment) and $\mathbf{N}^{t_1}(t)$ (denoted by G^{t_1} in

Equation (40), capturing dynamics following drug treatment at time t_1):

$$\begin{aligned}
\mathbb{E} [z^{N_H(t)}] &= \begin{cases} G(t, z_1 = z, \dots, z_k = z, z_{NL} = z, z_A = 1, z_D = 1, z_C = 1, z_P = 1, z_{PC} = 1) & \text{if } t < t_1 \\ G^{t_1}(t, z_1 = z, \dots, z_k = z, z_{NL} = z, z_A = 1, z_D = 1, z_C = 1, z_P = 1, z_{PC} = 1) & \text{if } t \geq t_1 \end{cases} \\
&= \begin{cases} \exp \left\{ -m(t) + \int_0^t \frac{\lambda(\tau)}{1+\nu(1-z)p_H(t-\tau)} d\tau \right\} & \text{if } t < t_1 \\ \exp \left\{ -m(t) + \int_0^{t_1} \frac{\lambda(\tau)}{1+\nu(1-p_{\text{rad}})(1-z)p_H(t-\tau)} d\tau + \int_{t_1}^t \frac{\lambda(\tau)}{1+\nu(1-z)p_H(t-\tau)} d\tau \right\} & \text{if } t \geq t_1 \end{cases} \\
&= \exp\{-m(t) + \ell(z, t)\} \tag{53}
\end{aligned}$$

where

$$\ell(z, t) = \begin{cases} \int_0^t \frac{\lambda(\tau)}{1+\nu(1-z)p_H(t-\tau)} d\tau & \text{if } t < t_1 \\ \int_0^{t_1} \frac{\lambda(\tau)}{1+\nu(1-p_{\text{rad}})(1-z)p_H(t-\tau)} d\tau + \int_{t_1}^t \frac{\lambda(\tau)}{1+\nu(1-z)p_H(t-\tau)} d\tau & \text{if } t \geq t_1. \end{cases}$$

From the PGF given by Equation (53), using Leibiniz integral rule, we can also compute the expected size of the hypnozoite reservoir

$$\begin{aligned}
\mathbb{E}[N_H(t)] &= \left. \frac{\partial \mathbb{E}[z^{N_H(t)}]}{\partial z} \right|_{z=1} \\
&= \begin{cases} \nu \int_0^t \lambda(\tau) p_H(t-\tau) d\tau & \text{if } t < t_1 \\ \nu(1-p_{\text{rad}}) \int_0^{t_1} \lambda(\tau) p_H(t-\tau) d\tau + \nu \int_{t_1}^t \lambda(\tau) p_H(t-\tau) d\tau & \text{if } t \geq t_1, \end{cases} \tag{54}
\end{aligned}$$

and the variance

$$\begin{aligned}
\text{Var}(N_H(t)) &= \left. \frac{\partial^2 \mathbb{E}[z^{N_H(t)}]}{\partial z^2} \right|_{z=1} + \left. \frac{\partial \mathbb{E}[z^{N_H(t)}]}{\partial z} \right|_{z=1} - \left(\left. \frac{\partial \mathbb{E}[z^{N_H(t)}]}{\partial z} \right|_{z=1} \right)^2 \\
&= \begin{cases} \int_0^t 2\lambda(\tau) (\nu p_H(t-\tau))^2 + \nu \lambda(\tau) p_H(t-\tau) d\tau & \text{if } t < t_1 \\ \int_0^{t_1} 2\lambda(\tau) (\nu(1-p_{\text{rad}}) p_H(t-\tau))^2 + \nu(1-p_{\text{rad}}) \lambda(\tau) p_H(t-\tau) d\tau \\ + \int_{t_1}^t 2\lambda(\tau) (\nu p_H(t-\tau))^2 + \nu \lambda(\tau) p_H(t-\tau) d\tau. & \text{if } t \geq t_1 \end{cases} \tag{55}
\end{aligned}$$

To invert the PGF given by Equation (53), we apply Faà di Bruno's formula (Di Bruno 1857), allowing us to recover the PMF for $N_H(t)$ in terms of partial Bell polynomials B_k^n :

$$\begin{aligned}
P(N_H(t) = n) &= \frac{e^{-m(t)}}{n!} \left. \frac{d}{dz^n} \exp\{\ell(z, t)\} \right|_{z=0} \\
&= \frac{\exp\{\ell(0, t) - m(t)\}}{n!} \sum_{k=1}^n B_{n,k} \left(\frac{\partial \ell}{\partial z}(0, t), \frac{\partial^2 \ell}{\partial z^2}(0, t), \dots, \frac{\partial^{n-k+1} \ell}{\partial z^{n-k+1}}(0, t) \right), \tag{56}
\end{aligned}$$

where by Leibinz integral rule and the geometric summation, we have that

$$\frac{\partial^k l}{\partial z^k}(0, t) = \begin{cases} \nu^k k! \int_0^t \frac{\lambda(\tau) p_H(t-\tau)^k}{[1+\nu p_H(t-\tau)]^{k+1}} d\tau & \text{if } t < t_1 \\ \nu^k k! \int_0^{t_1} \frac{\lambda(\tau) p_H(t-\tau)^k}{[1+\nu p_H(t-\tau)]^{k+1}} d\tau + \nu^k k! \int_{t_1}^t \frac{\lambda(\tau) (1-p_{\text{rad}})^k p_H(t-\tau)^k}{[1+\nu(1-p_{\text{rad}}) p_H(t-\tau)]^{k+1}} d\tau & \text{if } t \geq t_1. \end{cases} \quad (57)$$

4.1.1 Special Case: Short-Latency Hypnozoites, Constant Bite Rate

In the simplest case, where we consider short-latency hypnozoites ($k = 0$) and a constant bite rate $\lambda(t) = \lambda$ in the absence of radical cure, the PGF for the size of the hypnozoite reservoir at time t can be evaluated (Equation (53) in closed form

$$\mathbb{E} [z^{N_H(t)}] = \left(\frac{1 + \nu(1-z)e^{-(\alpha+\mu)t}}{1 + \nu(1-z)} \right)^{\frac{\lambda}{\alpha+\mu}}. \quad (58)$$

To compute the steady state distribution of N_H^* , we take the limit $t \rightarrow \infty$ in Equation (58)

$$\mathbb{E} [z^{N_H^*}] = (1 + \nu - \nu z)^{-\frac{\lambda}{\alpha+\mu}}. \quad (59)$$

Using the generalised binomial theorem, the PGF given by Equation (59) can be inverted to yield the PMF for the size of the hypnozoite reservoir at steady state

$$P(N_H^* = n) = \frac{1}{n!} \frac{\nu^n}{(1 + \nu)^{n + \frac{\lambda}{\alpha+\mu}}} \left(\frac{\lambda}{\alpha + \mu} + n - 1 \right)_{(n)} \quad (60)$$

where $(x)_{(n)}$ denotes the Pochhammer symbol.

4.1.2 Hypnozoite Reservoir Conditional on Infection Status

We can also characterise the size of the hypnozoite reservoir conditional on the current infection status. Here, we revert to the general setting of a time-dependent bite rate $\lambda(t)$ and either short- or long-latency hypnozoites ($k \geq 0$). Suppose an individual does not have a blood-stage infection at time t , that is, $N_A(t) = N_P(t) = 0$. By Xekalaki (1987), the conditional PGF for the size of the hypnozoite reservoir at time t , $N_H(t)$, can be obtained from the joint PGFs given by Equations (39) and (40) as follows:

$$\begin{aligned} \mathbb{E} [z^{N_H(t)} | N_A(t) = N_P(t) = 0] &= \begin{cases} \frac{G(z_1=z, \dots, z_k=z, z_{NL}=z, z_A=0, z_D=1, z_C=1, z_P=0, z_{PC}=1)}{G(z_1=1, \dots, z_k=1, z_{NL}=1, z_A=0, z_D=1, z_C=1, z_P=0, z_{PC}=1)} & \text{if } t < t_1 \\ \frac{G^{t_1}(z_1=z, \dots, z_k=z, z_{NL}=z, z_A=0, z_D=1, z_C=1, z_P=0, z_{PC}=1)}{G^{t_1}(z_1=1, \dots, z_k=1, z_{NL}=1, z_A=0, z_D=1, z_C=1, z_P=0, z_{PC}=1)} & \text{if } t \geq t_1 \end{cases} \\ &= \exp \{g(z, t) - g(1, t)\} \end{aligned} \quad (61)$$

where we define

$$g(z, t) = \begin{cases} \int_0^t \frac{\lambda(\tau)(1-p_{\text{prim}}e^{-\gamma(t-\tau)})}{1+\nu p_H(t-\tau)(1-z)+\nu p_A(t-\tau)} d\tau & \text{if } t < t_1 \\ \int_{t_1}^t \frac{\lambda(\tau)(1-p_{\text{prim}}e^{-\gamma(t-\tau)})}{1+\nu p_H(t-\tau)(1-z)+\nu p_A(t-\tau)} d\tau + \int_0^{t_1} \frac{\lambda(\tau)(1-p_{\text{prim}}(1-p_{\text{blood}})e^{-\gamma(t-\tau)})}{1+\nu p_H^r(t-\tau, t_1-\tau)(1-z)+\nu p_A^r(t-\tau, t_1-\tau)} d\tau & \text{if } t \geq t_1 \end{cases}.$$

As before, the expected size of the hypnozoite reservoir in an uninfected individual can be obtained from Equation (61) using Leibniz integral rule

$$\begin{aligned} \mathbb{E}[N_H(t)|N_A(t) = N_P(t) = 0] &= \left. \frac{\partial \mathbb{E}[z^{N_H(t)}|N_A(t) = N_P(t) = 0]}{\partial z} \right|_{z=1} \\ &= \begin{cases} \nu \int_0^t \frac{\lambda(\tau)p_H(t-\tau)(1-p_{\text{prim}}e^{-\gamma(t-\tau)})}{[1+\nu p_A(t-\tau)]^2} d\tau & \text{if } t < t_1 \\ \nu(1-p_{\text{rad}}) \int_0^{t_1} \frac{\lambda(\tau)p_H(t-\tau)(1-p_{\text{prim}}e^{-\gamma(t-\tau)})}{[1+\nu p_A^r(t-\tau, t_1-\tau)]^2} d\tau + \nu \int_{t_1}^t \frac{\lambda(\tau)p_H(t-\tau)(1-p_{\text{prim}}e^{-\gamma(t-\tau)})}{[1+\nu p_A(t-\tau)]^2} d\tau & \text{if } t \geq t_1. \end{cases} \end{aligned} \quad (62)$$

Similarly, we use Faà di Bruno's formula (Di Bruno 1857) to invert the conditional PGF given by Equation (61) and obtain the conditional probability masses for $N_H(t)$, given an individual does not have an ongoing blood-stage infection at time t :

$$\begin{aligned} P(N_H(t) = n|N_A(t) = N_P(t) = 0) &= \frac{1}{n!} \frac{\partial}{\partial z^n} \exp \{g(z, t) - g(1, t)\} \Big|_{z=0} \\ &= \frac{\exp \{g(0, t) - g(1, t)\}}{n!} \sum_{k=1}^n B_{n,k} \left(\frac{\partial g}{\partial z}(0, t), \frac{\partial^2 g}{\partial z^2}(0, t), \dots, \frac{\partial^{n-k+1} g}{\partial z^{n-k+1}}(0, t) \right) \end{aligned} \quad (63)$$

where, by Leibniz integral rule and the geometric summation, we have that

$$\frac{\partial^k g}{\partial z^k}(0, t) = \begin{cases} \nu^k k! \int_0^t \frac{\lambda(\tau)(1-p_{\text{prim}}e^{-\gamma(t-\tau)})p_H(t-\tau)^k}{[1+\nu(p_H(t-\tau)+p_A(t-\tau))]^{k+1}} d\tau & \text{if } t < t_1 \\ \nu^k k! \left(\int_{t_1}^t \frac{\lambda(\tau)(1-p_{\text{prim}}e^{-\gamma(t-\tau)})p_H(t-\tau)^k}{[1+\nu(p_H(t-\tau)+p_A(t-\tau))]^{k+1}} d\tau \right. & \text{if } t \geq t_1 \\ \left. + \int_{t_1}^t \frac{\lambda(\tau)(1-p_{\text{prim}}(1-p_{\text{blood}})e^{-\gamma(t-\tau)})p_H^r(t-\tau, t_1-\tau)^k}{[1+\nu(p_H^r(t-\tau, t_1-\tau)+p_A^r(t-\tau, t_1-\tau))]^{k+1}} d\tau \right) & \end{cases} \quad (64)$$

The conditional PMF for the size of the hypnozoite reservoir at time t , $N_H(t)$, given an ongoing blood stage infection at time t , that is, $N_A(t) + N_P(t) > 0$, follows readily from Equations (63) and (68) (see Section 4.2)

$$\begin{aligned} P(N_H(t) = n|N_A(t) + N_P(t) > 0) &= \frac{P(N_H(t) = n) - P(N_H(t) = n|N_A(t) = N_P(t) = 0)P(N_A(t) = N_P(t) = 0)}{1 - P(N_A(t) = N_P(t) = 0)} \end{aligned} \quad (65)$$

4.2 Probability of Infection

Prior to the establishment of a hypnozoite reservoir, primary infections are likely to be the dominant source of infection for an individual in an endemic setting. As the hypnozoite reservoir

accrues over time, we expect relapses to contribute to an increasingly large proportion of the infection burden; however, we expect primary infections to once again become the dominant source of infection if the hypnozoite reservoir is substantially reduced due to radical cure. We thus begin by examining the probability of relapse and primary infection both before and after the administration of drug treatment.

From the joint PGFs for $\mathbf{N}(t)$, (denoted G in Equation (39)), which holds prior to drug treatment, and $\mathbf{N}^{t_1}(t)$, (denoted G^{t_1} in Equation (40)), which holds after drug treatment at time t_1 , the probability that an individual does not have an ongoing primary infection at time t is

$$\begin{aligned}
P(N_P(t) = 0) &= \mathbb{E} [z^{N_P(t)}] \Big|_{z=0} \\
&= \begin{cases} G(t, z_1 = 1, \dots, z_k = 1, z_{NL} = 1, z_A = 1, z_D = 1, z_C = 1, z_P = 0, z_{PC} = 1) & \text{if } t < t_1 \\ G^{t_1}(t, z_1 = 1, \dots, z_k = 1, z_{NL} = 1, z_A = 1, z_D = 1, z_C = 1, z_P = 0, z_{PC} = 1) & \text{if } t \geq t_1 \end{cases} \\
&= \begin{cases} \exp \left\{ -p_{\text{prim}} \int_0^t \lambda(\tau) e^{-\gamma(t-\tau)} d\tau \right\} & \text{if } t < t_1 \\ \exp \left\{ -p_{\text{prim}} \left[\int_{t_1}^t \lambda(\tau) e^{-\gamma(t-\tau)} d\tau + (1 - p_{\text{blood}}) \int_0^{t_1} \lambda(\tau) e^{-\gamma(t-\tau)} \right] \right\} & \text{if } t \geq t_1. \end{cases} \quad (66)
\end{aligned}$$

Similarly, the probability that the individual does not have an ongoing relapse at time t is

$$\begin{aligned}
P(N_A(t) = 0) &= \mathbb{E} [z^{N_A(t)}] \Big|_{z=0} \\
&= \begin{cases} G(t, z_1 = 1, \dots, z_k = 1, z_{NL} = 1, z_A = 0, z_D = 1, z_C = 1, z_P = 1, z_{PC} = 1) & \text{if } t < t_1 \\ G^{t_1}(t, z_1 = 1, \dots, z_k = 1, z_{NL} = 1, z_A = 0, z_D = 1, z_C = 1, z_P = 1, z_{PC} = 1) & \text{if } t \geq t_1 \end{cases} \\
&= \begin{cases} \exp \left\{ -m(t) + \int_0^t \frac{\lambda(\tau)}{1 + \nu p_A(t-\tau)} d\tau \right\} & \text{if } t < t_1 \\ \exp \left\{ -m(t) + \int_{t_1}^t \frac{\lambda(\tau)}{1 + \nu p_A(t-\tau)} d\tau + \int_0^{t_1} \frac{\lambda(\tau)}{1 + \nu p_A^r(t-\tau, t_1-\tau)} d\tau \right\} & \text{if } t \geq t_1. \end{cases} \quad (67)
\end{aligned}$$

The probability that the individual is neither experiencing a relapse, nor a primary infection at time t is given by

$$\begin{aligned}
P(N_A(t) = 0, N_P(t) = 0) &= \mathbb{E} [z^{N_P(t) + N_A(t)}] \Big|_{z=0} \\
&= \begin{cases} G(t, z_1 = 1, \dots, z_k = 1, z_{NL} = 1, z_A = 0, z_D = 1, z_C = 1, z_P = 0, z_{PC} = 1) & \text{if } t < t_1 \\ G^{t_1}(t, z_1 = 1, \dots, z_k = 1, z_{NL} = 1, z_A = 0, z_D = 1, z_C = 1, z_P = 0, z_{PC} = 1) & \text{if } t \geq t_1 \end{cases} \\
&= \begin{cases} \exp \left\{ -m(t) + \int_0^t \frac{\lambda(\tau)(1 - p_{\text{prim}} e^{-\gamma(t-\tau)})}{1 + \nu p_A(t-\tau)} d\tau \right\} & \text{if } t < t_1 \\ \exp \left\{ -m(t) + \int_{t_1}^t \frac{\lambda(\tau)(1 - p_{\text{prim}} e^{-\gamma(t-\tau)})}{1 + \nu p_A(t-\tau)} d\tau + \int_0^{t_1} \frac{\lambda(\tau)(1 - p_{\text{prim}}(1 - p_{\text{blood}}) e^{-\gamma(t-\tau)})}{1 + \nu p_A^r(t-\tau, t_1-\tau)} d\tau \right\} & \text{if } t \geq t_1. \end{cases} \quad (68)
\end{aligned}$$

Equations (66) to (68) allow us to obtain several parameters describing the relative contributions of relapses and primary infections to blood-stage infection, noting that hypnozoite activation events in close proximity to mosquito bites can result in a multiple infections consisting of overlapping relapses and primary infections. Suppose an individual has an ongoing blood-stage infection at time t , that is, $\{N_A(t) + N_P(t) > 0\}$. We can compute the probability that the blood-stage infection is due to

- Hypnozoite activation (i.e. relapse) only:

$$P(N_P(t) = 0, N_A(t) > 0 | N_P(t) + N_A(t) > 0) = \frac{P(N_P(t) = 0) - P(N_P(t) = N_A(t) = 0)}{1 - P(N_P(t) = N_A(t) = 0)} \quad (69)$$

- Reinfection (i.e. primary infection) only:

$$P(N_P(t) > 0, N_A(t) = 0 | N_P(t) + N_A(t) > 0) = \frac{P(N_A(t) = 0) - P(N_P(t) = N_A(t) = 0)}{1 - P(N_P(t) = N_A(t) = 0)} \quad (70)$$

- Hypnozoite activation and reinfection (i.e. overlapping relapse and primary infection):

$$\begin{aligned} &P(N_P(t) > 0, N_A(t) > 0 | N_P(t) + N_A(t) > 0) \\ &= \frac{1 - P(N_P(t) = 0) - P(N_A(t) = 0) + P(N_P(t) = N_A(t) = 0)}{1 - P(N_P(t) = N_A(t) = 0)} \end{aligned} \quad (71)$$

4.3 Multiple Infections

Hypnozoite activation or reinfection events in quick succession may give rise to overlapping blood-stage infections, which can involve the co-circulation of genetically-distinct parasite strains in the bloodstream (Fola et al. 2017). Here, we assume that each primary infection is comprised of a single parasite strain, while hypnozoites are all genetically heterologous. The multiplicity of infection (MOI) is therefore given by the total number of active infections (i.e. primary infections and relapses) at time t : $M_I(t) := N_A(t) + N_P(t)$. Using the joint PGFs for $\mathbf{N}(t)$ (denoted G in Equation (39)), which holds prior to drug treatment and $\mathbf{N}^{t_1}(t)$ (denoted G^{t_1} in Equation (40)),

which holds following drug treatment at time t_1 , the PGF for $M_I(t)$ is given by

$$\begin{aligned} \mathbb{E}[z^{M_I(t)}] &= \begin{cases} G(t, z_1 = 1, \dots, z_k = 1, z_{NL} = 1, z_A = z, z_D = 1, z_C = 1, z_P = z, z_{PC} = 1) & \text{if } t < t_1 \\ G^{t_1}(t, z_1 = 1, \dots, z_k = 1, z_{NL} = 1, z_A = z, z_D = 1, z_C = 1, z_P = z, z_{PC} = 1) & \text{if } t \geq t_1 \end{cases} \\ &= \begin{cases} \exp \left\{ -m(t) + \int_0^t \lambda(\tau) \frac{z p_{\text{prim}} e^{-\gamma(t-\tau)} + (1-p_{\text{prim}}) e^{-\gamma(t-\tau)}}{1 + \nu p_A(t-\tau)(1-z)} d\tau \right\} & \text{if } t < t_1 \\ \exp \left\{ -m(t) + \int_{t_1}^t \lambda(\tau) \frac{z p_{\text{prim}} e^{-\gamma(t-\tau)} + (1-p_{\text{prim}}) e^{-\gamma(t-\tau)}}{1 + \nu p_A(t-\tau)(1-z)} d\tau \right. \\ \quad \left. + \int_0^{t_1} \lambda(\tau) \frac{z p_{\text{prim}}(1-p_{\text{blood}}) e^{-\gamma(t-\tau)} + (1-p_{\text{prim}}(1-p_{\text{blood}})) e^{-\gamma(t-\tau)}}{1 + \nu p_A^r(t-\tau, t_1-\tau)(1-z)} d\tau \right\} & \text{if } t \geq t_1 \end{cases} \\ &= \exp\{-m(t) + f(z, t)\}, \end{aligned} \tag{72}$$

where we denote

$$f(z, t) = \begin{cases} \int_0^t \lambda(\tau) \frac{z p_{\text{prim}} e^{-\gamma(t-\tau)} + (1-p_{\text{prim}}) e^{-\gamma(t-\tau)}}{1 + \nu p_A(t-\tau)(1-z)} d\tau & \text{if } t < t_1 \\ \int_{t_1}^t \lambda(\tau) \frac{z p_{\text{prim}} e^{-\gamma(t-\tau)} + (1-p_{\text{prim}}) e^{-\gamma(t-\tau)}}{1 + \nu p_A(t-\tau)(1-z)} d\tau \\ \quad + \int_0^{t_1} \lambda(\tau) \frac{z p_{\text{prim}}(1-p_{\text{blood}}) e^{-\gamma(t-\tau)} + (1-p_{\text{prim}}(1-p_{\text{blood}})) e^{-\gamma(t-\tau)}}{1 + \nu p_A^r(t-\tau, t_1-\tau)(1-z)} d\tau & \text{if } t \geq t_1 \end{cases}$$

To recover the probability mass function for $M_I(t)$ from the PGF given in Equation (72), we use a similar procedure to that in Section 4.1. By Faà di Bruno's formula (Di Bruno 1857), we have that

$$\begin{aligned} P(M_I(t) = n) &= \frac{e^{-m(t)}}{n!} \frac{d^n}{dz^n} \exp\{f(z, t)\} \Big|_{z=0} \\ &= \frac{\exp\{f(0, t) - m(t)\}}{n!} \sum_{k=1}^n B_{n,k} \left(\frac{\partial f}{\partial z}(0, t), \frac{\partial^2 f}{\partial z^2}(0, t), \dots, \frac{\partial f^{(n-k+1)}}{\partial z^{(n-k+1)}}(0, t) \right) \end{aligned} \tag{73}$$

where B_k^n denote the partial Bell polynomials and by Leibinz integral rule,

$$\begin{aligned} \frac{\partial^k f}{\partial z^k}(0, t) &= \begin{cases} k! \int_0^t \frac{\lambda(\tau) [\nu p_A(t-\tau)]^{k-1}}{[1 + \nu p_A(t-\tau)]^k} \left(p_{\text{prim}} e^{-\gamma(t-\tau)} + \frac{\nu p_A(t-\tau)(1-p_{\text{prim}}) e^{-\gamma(t-\tau)}}{1 + \nu p_A(t-\tau)} \right) d\tau & \text{if } t < t_1 \\ k! \left(\int_{t_1}^t \frac{\lambda(\tau) [\nu p_A(t-\tau)]^{k-1}}{[1 + \nu p_A(t-\tau)]^k} \left(p_{\text{prim}} e^{-\gamma(t-\tau)} + \frac{\nu p_A(t-\tau)(1-p_{\text{prim}}) e^{-\gamma(t-\tau)}}{1 + \nu p_A(t-\tau)} \right) d\tau \right. \\ \quad \left. + \int_0^{t_1} \frac{\lambda(\tau) [\nu p_A(t-\tau)]^{k-1}}{[1 + \nu p_A(t-\tau)]^k} \left(p_{\text{prim}}(1-p_{\text{blood}}) e^{-\gamma(t-\tau)} + \frac{\nu p_A(t-\tau)(1-p_{\text{prim}}(1-p_{\text{blood}})) e^{-\gamma(t-\tau)}}{1 + \nu p_A(t-\tau)} \right) d\tau \right) & \text{if } t \geq t_1 \end{cases} \\ & \tag{74} \end{aligned}$$

4.4 Time to First Recurrence

Next, we consider the time to first recurrence following drug treatment, a quantity that has been surveyed in longitudinal epidemiological studies across a range of transmission settings (Robinson et al. 2015; Taylor et al. 2019; Corder et al. 2020). Randomised controlled trials, comparing the time to first recurrence following treatment with radical cure compared to blood-

stage treatment only, have also been used to quantify the efficacy of radical cure (Nelwan et al. 2015).

Evaluating the PGF for the number of recurrences following drug treatment (Equation (52)) at $z = 0$ yields the probability of no recurrences in the interval $[t_1, t_2]$, given drug treatment is administered at time t_1 :

$$\begin{aligned} P(I_C(t_2) - I_C(t_1) = 0) &= \mathbb{E} [z^{I_C(t_2) - I_C(t_1)}] \Big|_{z=0} \\ &= \exp \left\{ -m(t_2) + \int_0^{t_1} \frac{\lambda(\tau)}{1 + \nu(1 - p_{\text{rad}})(B(t_2 - \tau) - B(t_1 - \tau))} d\tau + \int_{t_1}^{t_2} \frac{\lambda(\tau)(1 - p_{\text{prim}})}{1 + \nu B(t_2 - \tau)} d\tau \right\}. \end{aligned} \quad (75)$$

Since recurrences include both primary infections and relapses, setting $p_{\text{prim}} = 0$ in Equation (75) yields the distribution for the time to first relapse following drug treatment.

4.5 Cumulative Number of Infections Over Time

To quantify the longer-term impacts of a single administration of radical cure, we seek to compare the infection burden following radical cure, as opposed to blood-stage treatment only. Here, we consider the cumulative number of infections experienced in the interval $(t_1, t_2]$, following drug treatment at time t_1 , $I_C(t_2) - I_C(t_1)$. The PGF for $I_C(t_2) - I_C(t_1)$ (Equation (52)) can be written

$$\mathbb{E} [z^{I_C(t_2) - I_C(t_1)}] = \exp\{-m(t_2) + h(z, t_1, t_2)\}$$

where

$$h(z, t_1, t_2) = \int_0^{t_1} \frac{\lambda(\tau)}{1 + \nu(1 - p_{\text{rad}})[B(t_2 - \tau) - B(t_1 - \tau)](1 - z)} d\tau + \int_{t_1}^{t_2} \frac{\lambda(\tau)[1 - p_{\text{prim}} + zp_{\text{prim}}]}{1 + \nu B(t_2 - \tau)(1 - z)} d\tau.$$

We can thus compute the expected number of infections following drug treatment

$$\begin{aligned} \mathbb{E}[I_C(t_2) - I_C(t_1)] &= \frac{\partial \mathbb{E}[z^{I_C(t_2) - I_C(t_1)}]}{\partial z} \Big|_{z=1} \\ &= \nu(1 - p_{\text{rad}}) \int_0^{t_1} \lambda(\tau)(B(t_2 - \tau) - B(t_1 - \tau)) d\tau + \int_{t_1}^{t_2} \lambda(\tau)(p_{\text{prim}} + \nu B(t_2 - \tau)) d\tau, \end{aligned} \quad (76)$$

as well as the variance

$$\begin{aligned} \text{Var}(I_C(t_2) - I_C(t_1)) &= \frac{\partial^2 \mathbb{E}[z^{I_C(t_2) - I_C(t_1)}]}{\partial z^2} \Big|_{z=1} + \frac{\partial \mathbb{E}[z^{I_C(t_2) - I_C(t_1)}]}{\partial z} \Big|_{z=1} - \left(\frac{\partial \mathbb{E}[z^{I_C(t_2) - I_C(t_1)}]}{\partial z} \Big|_{z=1} \right)^2 \\ &= \int_0^{t_1} \lambda(\tau) \left[2(\nu(1 - p_{\text{rad}})(B(t_2 - \tau) - B(t_1 - \tau)))^2 + \nu(1 - p_{\text{rad}})(B(t_2 - \tau) - B(t_1 - \tau)) \right] d\tau \\ &\quad + \int_{t_1}^{t_2} \lambda(\tau) \left[2(\nu B(t_2 - \tau))^2 + (2p_{\text{prim}} + 1)\nu B(t_2 - \tau) + p_{\text{prim}} \right] d\tau. \end{aligned} \quad (77)$$

As in Section 4.1, we can invert the PGF in Equation (52) to yield the PMF for $I_C(t_2) - I_C(t_1)$ in terms of partial Bell polynomials B_k^n by applying Faà di Bruno's formula (Di Bruno 1857):

$$\begin{aligned} P(I_C(t_2) - I_C(t_1) = n) &= \frac{e^{-m(t_2)}}{n!} \frac{d^n}{dz^n} \exp \{h(z, t_1, t_2)\} \Big|_{z=0} \\ &= \frac{\exp \{h(0, t_1, t_2) - m(t_2)\}}{n!} \sum_{k=1}^n B_{n,k} \left(\frac{\partial h}{\partial z}(0, t_1, t_2), \frac{\partial^2 h}{\partial z^2}(0, t_1, t_2), \dots, \frac{\partial h^{(n-k+1)}}{\partial z^{(n-k+1)}}(0, t_1, t_2) \right) \end{aligned} \quad (78)$$

where, using Leibniz integral rule and the geometric series summation

$$\begin{aligned} \frac{\partial^k h}{\partial z^k} &= k! \int_{t_1}^{t_2} \frac{\lambda(\tau) [\nu B(t_2 - \tau)]^{k-1}}{[1 + \nu B(t_2 - \tau)]^k} \left(p_{\text{prim}} + \frac{\nu B(t_2 - \tau)(1 - p_{\text{prim}})}{1 + \nu B(t_2 - \tau)} \right) d\tau + \\ &\quad k! \int_0^{t_1} \frac{\lambda(\tau) [\nu(1 - p_{\text{rad}})(B(t_2 - \tau) - B(t_1 - \tau))]^k}{[1 + \nu(1 - p_{\text{rad}})(B(t_2 - \tau) - B(t_1 - \tau))]^{k+1}} d\tau. \end{aligned} \quad (79)$$

5 Illustrative Results

In Section 4, we derived several quantities of epidemiological significance pertaining to the dynamics of the hypnozoite reservoir and the infection burden in a general transmission setting. Comparing these dynamics following radical cure, as opposed to blood-stage treatment only, can help elucidate the epidemiological effects of radical cure. Here, we provide illustrative results for hypnozoite and infection dynamics for both short-latency (tropical) and long-latency (temperate) strains. For simplicity, we restrict our attention to a constant transmission setting.

5.1 Hypnozoite Distributions are Zero-Inflated at Early Times and in Low Transmission Settings

We begin by considering the size of the hypnozoite reservoir in the absence of drug treatment (Figure 7). Distributions for the total size of the hypnozoite reservoir (state H) are shown in blue; non-latent hypnozoites (state NL), which govern the risk of relapse but account for only

a subset of the reservoir for long-latency strains, are shown in orange. The progressive accrual of the hypnozoite reservoir in an intermediate transmission setting is demonstrated in Figures 7A and 7C. PMFs for the size of the hypnozoite reservoir are distinctly zero-inflated at early times, since, while each bite establishes a sizeable hypnozoite inoculum on average, there is a reasonably high probability of an individual having experienced no mosquito bites early on. Due to the enforced dormancy period, there is a delay of approximately six months before a non-latent hypnozoite reservoir starts to accumulate (Figure 7C). However, the hypnozoite reservoir, both latent and non-latent, eventually stabilises in size as the clearance of hypnozoites from the liver (through either death or activation) offsets replenishment of the reservoir through mosquito inoculation. In Figures 7B and 7D, we examine the equilibrium hypnozoite distribution ($t = 35$ years) across a range of biting intensities. For very low bite rates, we likewise observe zero-inflated distributions since the probability of a recent mosquito bite (relative to the expected duration of hypnozoite carriage) is comparatively low. Non-zero central tendencies emerge as the biting intensity increases and the number of recent bites contributing to the hypnozoite reservoir is expected to increase.

5.2 Multiple Infections are Driven By Relapses

Multiple (overlapping) infections can arise from reinfection and hypnozoite activation events in quick succession, with experimental data revealing polyclonal relapses even in the absence of reinfection (Popovici et al. 2018). Here, we characterise the relationship between the size of the hypnozoite reservoir; the prevalence of multiple infections, and the relative contribution of relapses to the infection burden. Figures 8A and 8D illustrate the expected size of the hypnozoite reservoir over time, with hypnozoite distributions expected to stabilise prior to the administration of drug treatment at $t_1 = 2.5$ years. In Figures 8B and 8E, we examine distributions for the multiplicity of infection (MOI) in a single individual, under the assumption that each primary infection is comprised of a single clone, while all hypnozoites are genetically heterologous (our definition of MOI is equivalent to the number of active infections at a given point in time under our model). The conditional probability of an active infection comprising of either a primary infection (brown), relapse (turquoise) or both (purple) is shown in Figures 8C and 8F.

Primary infections are initially the dominant source of infection (Figures 8C and 8F, solid brown line), as the hypnozoite reservoir is yet to accumulate (Figures 8A and 8D). There is thus a low initial probability of multiple infections ($\text{MOI} > 1$) since overlapping primary infections, arising from mosquito bites in quick succession, are unlikely to occur under the given bite rate (Figures

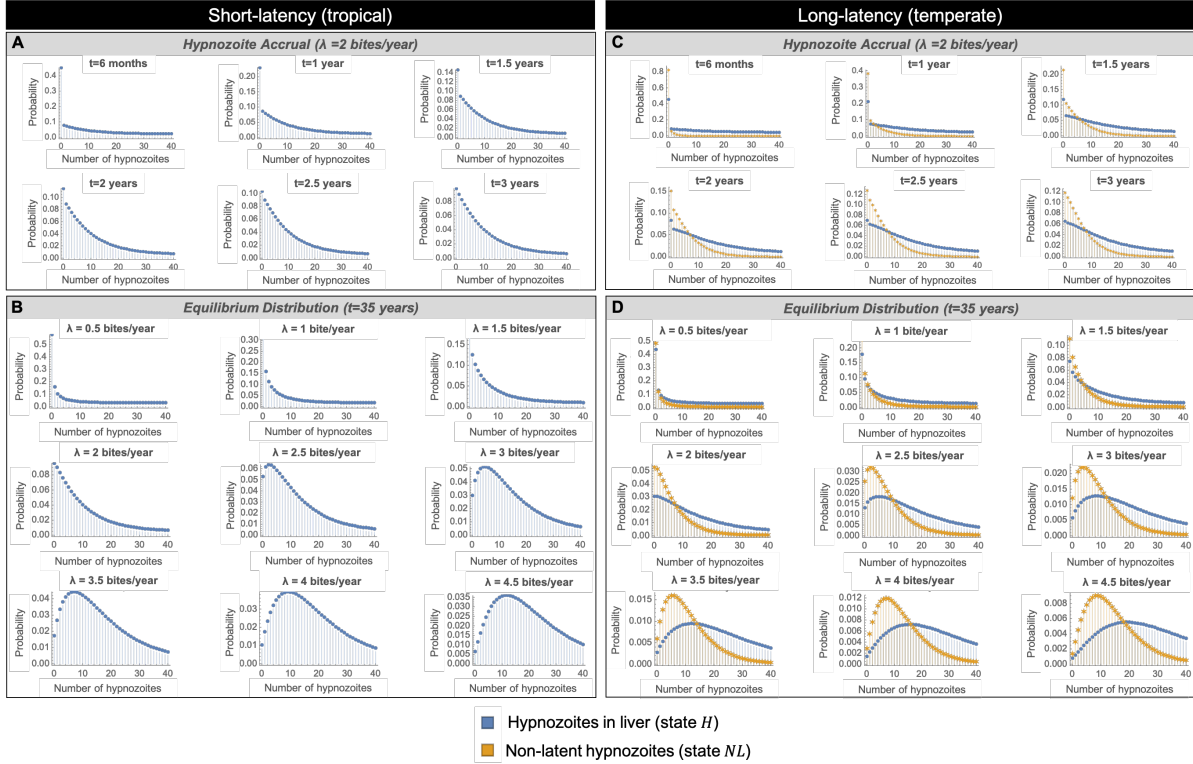


Figure 7: Distributions for the size of the hypnozoite reservoir in the absence of drug treatment (Equation (56)). The total number of hypnozoites in the liver (both latent and non-latent) are shown in blue, while non-latent hypnozoites are shown in orange. For long-latency strains, the hypnozoite reservoir is comprised of both latent hypnozoites (that may die, but not activate) and non-latent hypnozoites (that may either activate or die); for short-latency strains, all hypnozoites in the liver are subject to both death and activation (Section 2.1). In subplots A and C, we show the accrual of the hypnozoite reservoir over time ($t = 0.5, 1, 1.5, 2, 2.5, 3$ years) in a constant transmission setting with bite rate $\lambda = 2/365 \text{ day}^{-1}$. In subplots B and D, we show the equilibrium distribution ($t = 35$ years) for the size of the hypnozoite reservoir for various biting intensities ($\lambda = 0.5, 1, 1.5, 2, 2.5, 3, 3.5, 4, 4.5$ bites/year). Based on estimates from White, Karl, et al. (2014), we assume an average of $\nu = 9$ hypnozoites are established per bite. Hypnozoite activation and clearance rates, $\alpha = 1/334 \text{ day}^{-1}$, $\mu = 1/442 \text{ day}^{-1}$, and, in the case of long-latency strains, the number of latency compartments $k = 35$, as well as the rate of progression through successive hypnozoite strains $\delta = 1/5 \text{ day}^{-1}$, have been taken from White, Karl, et al. (2014).

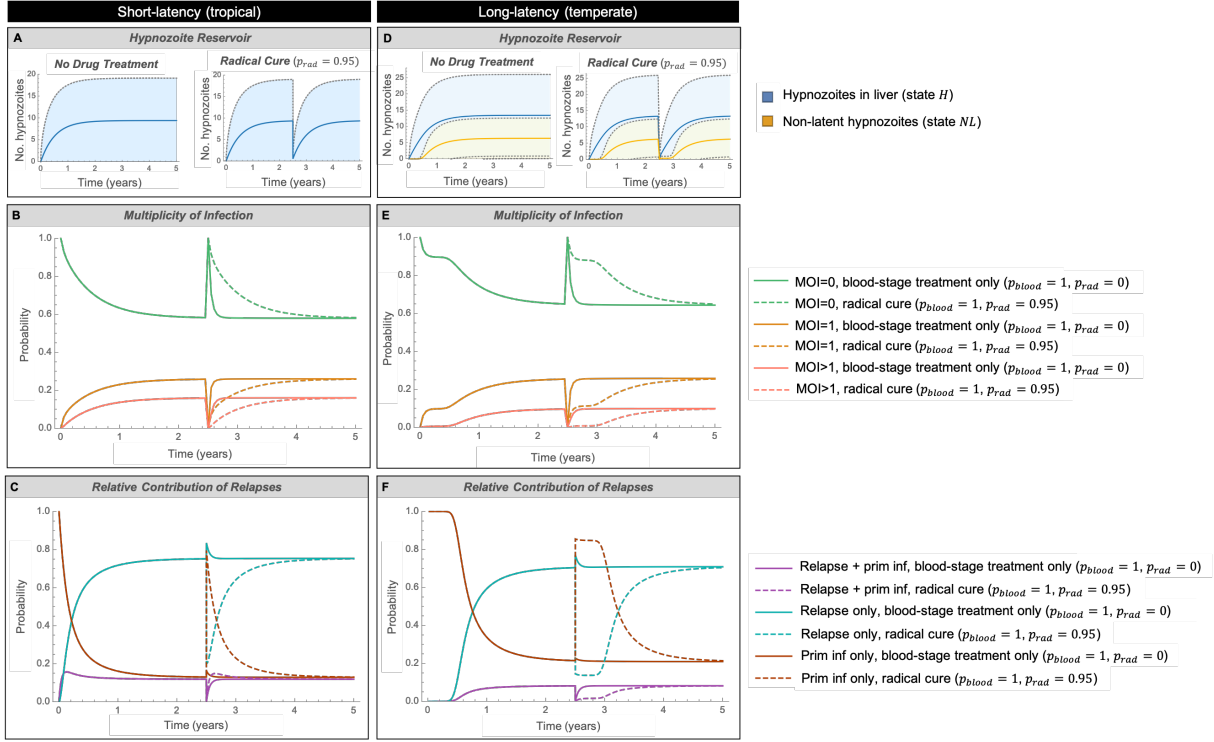


Figure 8: Hypnozoite and infection dynamics for an individual in a general transmission setting. At time zero, we assume an individual first enters an endemic setting. At time $t = 2.5$ years, we consider the administration of either radical cure (dotted lines, $p_{rad} = 0.95$, $p_{blood} = 1$) or blood-stage treatment only (solid lines, $p_{rad} = 0$, $p_{blood} = 1$). In subplots A and D, we show the expected size of the hypnozoite reservoir (Equation (54)), with shaded regions indicating one standard deviation above and below the mean (Equation (55)). Distributions for the multiplicity of infection, that is, the number of active infections $N_A(t) + N_P(t)$ over time (Equation (73)) are shown in subplots B and E. Given an ongoing infection (that is, $N_A(t) + N_P(t) > 0$), the probability of that infection comprising of a relapse only, primary infection only or overlapping relapses and primary infections (Equations (70), (69) and (71), computed using Equations (66), (67) and (68)) is shown in subplots C and F. Here, we assume a constant transmission setting with bite rate $\lambda = 2/365 \text{ day}^{-1}$ and all bites necessarily leading to a primary infection, that is, $p_{prim} = 1$. At baseline, we assume that each primary infection and relapse is cleared at rate $\gamma = 1/20 \text{ day}^{-1}$. Based on estimates from White, Karl, et al. (2014), we assume an average of $\nu = 9$ hypnozoites are established per bite. Hypnozoite activation and clearance rates, $\alpha = 1/334 \text{ day}^{-1}$, $\mu = 1/442 \text{ day}^{-1}$, and, in the case of long-latency strains, the number of latency compartments $k = 35$, as well as the rate of progression through successive hypnozoite strains $\delta = 1/5 \text{ day}^{-1}$, are from White, Karl, et al. (2014).

8B and 8E, solid red line). Given long-latency hypnozoites necessarily undergo a dormancy phase before they may activate, there is a delay of approximately six months before there is a non-negligible risk of relapse, during which we expect only primary infections (Figure 8F, solid brown line) with MOI=1 (Figure 8E, solid orange line). As the hypnozoite reservoir accrues and eventually stabilises in size (Figure 8A, Figure 8D), both the risk of multiple infections (MOI>1) (Figures 8B and 8E, solid red line) and the relative contributions of relapses to the infection burden (Figures 8C and 8F, solid turquoise line) rise steadily, before plateauing.

Upon the administration of drug treatment at time $t_1 = 2.5$ years after the individual first enters the endemic setting, all ongoing recurrences are instantaneously cleared. Since blood-stage treatment does not clear the hypnozoite reservoir, the probability of infection increases sharply to its original level within weeks of treatment (Figures 8B and 8E, solid lines), with relapses remaining the dominant source of infection (Figures 8C and 8F, solid turquoise line). Following treatment with radical cure, however, there is period during which primary infections dominate (Figures 8C and 8F, dotted brown line), which is longer for long-latency strains since hypnozoites must emerge from dormancy prior to activation; the risk of infection prior to drug treatment is only reached after a year has passed, when the hypnozoite reservoir is expected to have been replenished to its previous level (Figures 8A and 8D).

5.3 Heterogeneity in Recurrences Following Drug Treatment

To quantify the longer-term effects of a single administration of radical cure on the infection burden, we examine the cumulative number of recurrences following drug treatment (Figure 9). Since we do not account for a drug washout period, blood-stage treatment only ($p_{\text{rad}} = 0$) clears ongoing recurrences upon administration, but does not affect subsequent infections. Prior to drug treatment at $t_1 = 2.5$ years, we expect both the size of the hypnozoite reservoir (Figures 8A and 8D) and the probability of infection (Figures 8B and 8E, solid lines) to have largely stabilised. Accordingly, the expected number of recurrences following blood-stage treatment only at time $t_1 = 2.5$ years is approximately linear (Figures 9A1 and 9C1). However, distributions for the cumulative number of relapses following blood-stage treatment only (Figures 9B and 9D, blue curves) reveal substantial heterogeneity, arising from the batch arrival of hypnozoites for each bite; while infective bites are relatively infrequent, each bite establishes a reasonably large hypnozoite inoculum and thus contributes substantially to the relapse burden.

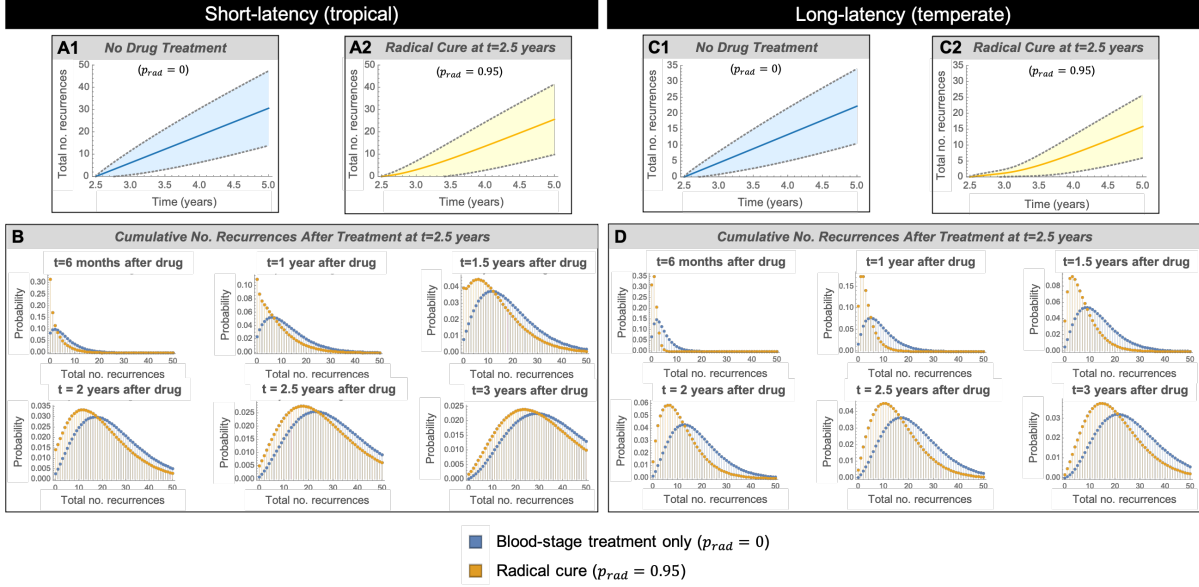


Figure 9: Distributions for the cumulative number of recurrences following drug treatment. In subplots A and C, we compare a scenario with no drug treatment (A1, C1) against the administration of reasonably efficacious radical cure ($p_{\text{rad}} = 0.95$) (A2, C2) at time $t_1 = 2.5$ years after an individual has been first exposed to an endemic setting; expected values (Equation (76)), with shaded regions indicating one standard deviation (Equation (77)) above and below the mean, are shown. For long-latency strains, a single administration of radical cure in this simulation is expected to prevent 6.4 relapses over a 2.5 year period following treatment, while for short-latency strains, we expect 5 relapses to be prevented. PMFs for the cumulative number of infections in the interval $(t_1, t_1 + t]$ following drug treatment (Equation (78)) are shown in subplots B and D for various time points ($t = 0.5, 1, 2, 5, 2, 2.5, 3$ years). Here, we assume a constant transmission setting with bite rate $\lambda = 2/365 \text{ day}^{-1}$ and all bites necessarily leading to a primary infection, that is, $p_{\text{prim}} = 1$. Model parameters ($\gamma, \mu, \alpha, k, \delta$) as per Figure 8.

Following treatment with radical cure, there is a delay before the hypnozoite reservoir is replenished, and consequently a period during which relapses are limited (Figures 8C and 8F, dotted lines). Hence, the expected number of recurrences following radical cure (Figures 9A2, 9C2) initially rises slowly due to primary infections dominating, but similarly becomes approximately linear as the hypnozoite reservoir accrues and stabilises in size (Figures 8A and 8D). For long-latency strains, the expected number of relapses grows slowly for a prolonged period (Figure 9C2) as each hypnozoite established in the liver must emerge from dormancy prior to contributing to the risk of relapse.

6 Discussion

The hypnozoite reservoir governs the epidemiology of *P. vivax*, with important implications for treatment and control. Radical curative therapies, which target the hypnozoite reservoir, have the potential to aid elimination efforts. Here, we have developed a stochastic within-host model to capture hypnozoite and infection dynamics for vivax malaria in a general transmission setting, whilst accounting for the administration of radical cure. We have proposed a relapse-clearance model adapted to both short- and long-latency hypnozoite strains, that extends previous models (White, Karl, et al. 2014; Mehra et al. 2020) to allow for drug treatment and an exponentially-distributed relapse following each hypnozoite activation event. Extending our previous work (Mehra et al. 2021) to concurrently monitor hypnozoite and infection dynamics, we have embedded our relapse-clearance model in an epidemiological framework capturing repeated mosquito inoculation. By constructing an open network of infinite server queues with batch arrivals, we have derived joint PGFs for the size of the hypnozoite reservoir and the cumulative number of infections over time, both in the absence of drug treatment (Equation (39)) and following the administration of radical cure (Equation (40)), yielding analytic distributions for several quantities of epidemiological significance.

Although the risk of relapse is dependent on the dynamics of the hypnozoite reservoir, a common approach across many statistical and transmission models has been an assumed distributional form for the risk of relapse (Ishikawa et al. 2003; Aguas, Ferreira, and Gomes 2012; Roy et al. 2013; Chamchod and Beier 2013; Lover et al. 2014; Robinson et al. 2015; White, Shirreff, et al. 2016; Taylor et al. 2019). Efforts to explicitly model the accrual of the hypnozoite reservoir, with clearance (through either death or activation) offsetting replenishment (through mosquito bites), have been more limited. By embedding an activation-clearance model for short-latency strains in a population-level transmission model allowing for variable hypnozoite inocula per

bite, White, Karl, et al. (2014) have obtained distributions for prevalence and the size of the hypnozoite reservoir under a range of control measures, including radical cure. Here, we jointly characterise within-host hypnozoite and infection dynamics for both short- and long-latency strains, whilst accounting for the effects of radical cure. To our knowledge, we provide the first analytical descriptions of several important epidemiological quantities, including the size of the hypnozoite reservoir; distributions of multiple infections; the relative contributions of primary infections to the infection burden and the cumulative number of infections over time. By describing the time evolution of the hypnozoite reservoir in a general transmission setting, we capture transient dynamics that are unlikely to be captured by an assumed distributional form, but provide insight into the epidemiological consequences of radical cure. Our model can be calibrated efficiently to data using the time to first recurrence following drug treatment, a frequently collected piece of epidemiological information (Robinson et al. 2015; Taylor et al. 2019; Corder et al. 2020) for which we provide explicit analytic formulae (Equation (75)). Our model thus has the potential to address questions around the heterogeneity of relapse risk in communities. While our within-host model provides insight into the epidemiological effects of radical cure on a single individual, population-level models are required to evaluate the utility of radical cure as a tool for elimination and control (Robinson et al. 2015; White, Walker, et al. 2018). Our analytic within-host distributions can be readily embedded in multiscale models to yield further insights.

Our model is underpinned by various simplifying assumptions. Similarly to White, Karl, et al. (2014) and Mehra et al. (2020), our relapse-clearance model for a single hypnozoite considers a baseline scenario, with spontaneous hypnozoite activation assumed to occur at a constant rate post-dormancy; we do not consider other possible mechanisms that have been hypothesised to temporarily elevate reactivation rates, such as systemic febrile illness (Shanks and White 2013) or bites from certain mosquito vectors (Hulden and Hulden 2011). We model drug treatment by assuming a fixed probability of survival for each hypnozoite, and a fixed probability of persistence for each blood-stage infection, under the assumption that the effects of drug treatment are instantaneous. Drug washout periods, with antimalarial half-lives ranging from approximately 40 minutes for artesunate (Morris et al. 2011), to 6 hours for primaquine (radical cure) (White 1992) and 30-60 days for chloroquine (White 1992), can be incorporated into our relapse-clearance framework using an appropriate forcing function. In fact, the form of the instantaneous forcing function in Equations (17) to (22) follows from taking the limit

$$\lim_{\Delta t \rightarrow 0} \eta(\Delta t)H(t - s_j)H(s_j + \Delta t - t) = \ln((1 - p)^{-1})\delta_D(t - s_j),$$

where H denotes the Heavyside step function (not to be confused with the hypnozoite state H); $\delta_D(\cdot)$ denotes the Dirac delta function (not to be confused with δ , a scalar parameter that denotes the rate of transition between successive latency compartments), and the rate constant $\eta(\Delta t)$ is chosen such that a drug causes a transition with probability p in the interval $(s_j, s_j + \Delta t)$

$$e^{-\eta(\Delta t)\Delta t} = 1 - p \iff \eta(\Delta t) = \frac{\ln((1-p)^{-1})}{\Delta t}.$$

While drug washout periods are an important consideration for interpreting data for the time to first recurrence, in this work, we have been concerned primarily with longer-term dynamics following drug treatment.

Although we account for multiple infections arising from reinfection (mosquito bites) or hypnozoite activation events in quick succession, our model does not capture the complexities of blood-stage infection. Under our framework, an infection refers to a period of parasitemia triggered by either by the activation of a single hypnozoite (relapse), or a single mosquito bite (primary infection); we model neither parasite densities, nor clinical disease status, over the course of each infection. The assumption that the duration of each infection is exponentially-distributed can be relaxed, but independent clearance of each infection is critical to our analytic framework; as such, our model is not equipped to capture phenomena like within-host competition between co-circulating strains (De Roode et al. 2005). Our model, moreover, does not account for the acquisition of immunity. While antimalarial immunity can modulate parasite clearance (Artavanis-Tsakonas, Tongren, and Riley 2003), we assume that the duration of each infection is identically-distributed. Given the progressive acquisition of immunity against clinical disease (clinical immunity), followed by the modulation of parasitemia (anti-parasite immunity) (Schofield and Mueller 2006), modelling immunity requires the coupling of our framework to mechanistic models of blood-stage infection. Since antimalarial immunity is strain-specific, albeit with cross-protectivity amongst strains (Mueller et al. 2013), strain structure is another important consideration; repeated exposure to a single strain, either through the activation of homologous hypnozoites or across multiple bites, can generate strong strain-specific immune protection, but partial protection against heterologous strains (Mueller et al. 2013), thereby modulating blood-stage dynamics. Modelling strain structure would also allow for precise distributions of MOI (here, we assume MOI to be given by the number of active infections at a given point in time, without accounting for the possibility of overlapping strains across infections, nor polyclonal primary infections).

Our work, nonetheless, characterises the dependence of infection dynamics for *P. vivax*, including

distributions of multiple infections, the relative contribution of relapses to the infection burden and the cumulative number of infections over time, on the accrual of the hypnozoite reservoir. By comparing the infection burden under in the absence of drug treatment against the administration of arbitrarily effective radical cure, our work contributes to the epidemiological understanding of the effects of radical cure on *P. vivax* malaria.

Acknowledgements

D. Khoury's research is supported by the Australian Research Council (ARC) (DP180103875) and the National Health and Medical Research Council (NHMRC) of Australia (1141921). J.M. McCaw's research is supported by the ARC (DP170103076). J.A. Flegg's research is supported by the ARC (DE160100227, DP200100747).

References

- Di Bruno, F Faà (1857). “Note sur une nouvelle formule de calcul différentiel”. In: *Quarterly J. Pure Appl. Math* 1.359-360, p. 12.
- Lewis, Peter AW (1967). “Non-homogeneous branching Poisson processes”. In: *Journal of the Royal Statistical Society: Series B (Methodological)* 29.2, pp. 343–354.
- Harrison, J Michael and Austin J Lemoine (1981). “A note on networks of infinite-server queues”. In: *Journal of Applied Probability*, pp. 561–567.
- Holman, DF, ML Chaudhry, and BRK Kashyap (1983). “On the service system $MX/G/\infty$ ”. In: *European Journal of Operational Research* 13.2, pp. 142–145.
- Xekalaki, Eydokia (1987). “A method for obtaining the probability distribution of m components conditional on ℓ components of a random sample”. In: *Rev. Roumaine Math. Pure Appl* 32, pp. 581–583.
- White, NJ (1992). “Antimalarial pharmacokinetics and treatment regimens.” In: *British Journal of Clinical Pharmacology* 34.1, pp. 1–10.
- Parzen, E (1999). “Stochastic Processes, Vol. 24”. In: *SIAM, Philadelphia, Pa, USA*.
- Artavanis-Tsakonas, K, JE Tongren, and EM Riley (2003). “The war between the malaria parasite and the immune system: immunity, immunoregulation and immunopathology”. In: *Clinical & Experimental Immunology* 133.2, pp. 145–152.
- Ishikawa, Hirofumi, Akira Ishii, Nobuhiko Nagai, Hiroshi Ohmae, Masakazu Harada, Setsuo Suguri, and Judson Leafasia (2003). “A mathematical model for the transmission of *Plasmodium vivax* malaria”. In: *Parasitology International* 52.1, pp. 81–93.
- De Roode, Jacobus C, Michelle EH Helinski, M Ali Anwar, and Andrew F Read (2005). “Dynamics of multiple infection and within-host competition in genetically diverse malaria infections”. In: *The American Naturalist* 166.5, pp. 531–542.
- Schofield, Louis and Ivo Mueller (2006). “Clinical immunity to malaria”. In: *Current Molecular Medicine* 6.2, pp. 205–221.
- Jeffrey, Alan and Daniel Zwillinger (2007). *Table of integrals, series, and products*. Elsevier.
- Wells, Timothy NC, Jeremy N Burrows, and J Kevin Baird (2010). “Targeting the hypnozoite reservoir of *Plasmodium vivax*: the hidden obstacle to malaria elimination”. In: *Trends in Parasitology* 26.3, pp. 145–151.
- Hulden, Lena and Larry Hulden (2011). “Activation of the hypnozoite: a part of *Plasmodium vivax* life cycle and survival”. In: *Malaria Journal* 10.1, pp. 1–6.
- Morris, Carrie A, Stephan Duparc, Isabelle Borghini-Fuhrer, Donald Jung, Chang-Sik Shin, and Lawrence Fleckenstein (2011). “Review of the clinical pharmacokinetics of artesunate and

- its active metabolite dihydroartemisinin following intravenous, intramuscular, oral or rectal administration”. In: *Malaria Journal* 10.1, pp. 1–17.
- Aguas, Ricardo, Marcelo U Ferreira, and M Gabriela M Gomes (2012). “Modeling the effects of relapse in the transmission dynamics of malaria parasites”. In: *Journal of Parasitology Research* 2012.
- Shanks, G Dennis (2012). “Control and elimination of *Plasmodium vivax*”. In: *Advances in Parasitology* 80, pp. 301–341.
- White, Nicholas J and Mallika Imwong (2012). “Relapse”. In: *Advances in Parasitology* 80, pp. 113–150.
- Chamchod, Farida and John C Beier (2013). “Modeling *Plasmodium vivax*: relapses, treatment, seasonality, and G6PD deficiency”. In: *Journal of Theoretical Biology* 316, pp. 25–34.
- Mueller, Ivo, Mary R Galinski, Takafumi Tsuboi, Myriam Arevalo-Herrera, William E Collins, and Christopher L King (2013). “Natural acquisition of immunity to *Plasmodium vivax*: epidemiological observations and potential targets”. In: *Advances in Parasitology*. Vol. 81. Elsevier, pp. 77–131.
- Roy, Manojit, Menno J Bouma, Edward L Ionides, Ramesh C Dhiman, and Mercedes Pascual (2013). “The potential elimination of *Plasmodium vivax* malaria by relapse treatment: insights from a transmission model and surveillance data from NW India”. In: *PLoS Neglected Tropical Diseases* 7.1, e1979.
- Shanks, G Dennis and Nicholas J White (2013). “The activation of vivax malaria hypnozoites by infectious diseases”. In: *The Lancet Infectious Diseases* 13.10, pp. 900–906.
- Battle, Katherine E et al. (2014). “Geographical variation in *Plasmodium vivax* relapse”. In: *Malaria Journal* 13.1, pp. 1–16.
- Lover, Andrew A, Xiahong Zhao, Zheng Gao, Richard J Coker, and Alex R Cook (2014). “The distribution of incubation and relapse times in experimental human infections with the malaria parasite *Plasmodium vivax*”. In: *BMC Infectious Diseases* 14.1, pp. 1–10.
- White, Michael T, Stephan Karl, Katherine E Battle, Simon I Hay, Ivo Mueller, and Azra C Ghani (2014). “Modelling the contribution of the hypnozoite reservoir to *Plasmodium vivax* transmission”. In: *eLife* 3, e04692.
- Kerlin, Douglas H and Michelle L Gatton (2015). “A simulation model of the within-host dynamics of *Plasmodium vivax* infection”. In: *Malaria Journal* 14.1, p. 51.
- Nelwan, Erni J et al. (2015). “Randomized trial of primaquine hypnozoitocidal efficacy when administered with artemisinin-combined blood schizontocides for radical cure of *Plasmodium vivax* in Indonesia”. In: *BMC Medicine* 13.1, pp. 1–12.

- Robinson, Leanne J et al. (2015). “Strategies for understanding and reducing the *Plasmodium vivax* and *Plasmodium ovale* hypnozoite reservoir in Papua New Guinean children: a randomised placebo-controlled trial and mathematical model”. In: *PLoS Med* 12.10, e1001891.
- WHO (2015). *Control and elimination of Plasmodium vivax malaria: a technical brief*. World Health Organization.
- Howes, Rosalind E, Katherine E Battle, Kamini N Mendis, David L Smith, Richard E Cibulskis, J Kevin Baird, and Simon I Hay (2016). “Global epidemiology of *Plasmodium vivax*”. In: *The American Journal of Tropical Medicine and Hygiene* 95.6_Suppl, pp. 15–34.
- Olliaro, Piero L et al. (2016). “Implications of *Plasmodium vivax* biology for control, elimination, and research”. In: *The American Journal of Tropical Medicine and Hygiene* 95.6_Suppl, pp. 4–14.
- White, Michael T, George Shirreff, Stephan Karl, Azra C Ghani, and Ivo Mueller (2016). “Variation in relapse frequency and the transmission potential of *Plasmodium vivax* malaria”. In: *Proceedings of the Royal Society B: Biological Sciences* 283.1827, p. 20160048.
- Fola, Abebe A et al. (2017). “Higher complexity of infection and genetic diversity of *Plasmodium vivax* than *Plasmodium falciparum* across all malaria transmission zones of Papua New Guinea”. In: *The American Journal of Tropical Medicine and Hygiene* 96.3, pp. 630–641.
- Popovici, Jean et al. (2018). “Genomic analyses reveal the common occurrence and complexity of *Plasmodium vivax* relapses in Cambodia”. In: *MBio* 9.1.
- White, Michael T, Patrick Walker, et al. (2018). “Mathematical modelling of the impact of expanding levels of malaria control interventions on *Plasmodium vivax*”. In: *Nature Communications* 9.1, pp. 1–10.
- Taylor, Aimee R et al. (2019). “Resolving the cause of recurrent *Plasmodium vivax* malaria probabilistically”. In: *Nature Communications* 10.1, pp. 1–11.
- Corder, Rodrigo M, Antonio CP de Lima, David S Khoury, Steffen S Docken, Miles P Davenport, and Marcelo U Ferreira (2020). “Quantifying and preventing *Plasmodium vivax* recurrences in primaquine-untreated pregnant women: An observational and modeling study in Brazil”. In: *PLoS Neglected Tropical Diseases* 14.7, e0008526.
- Mehra, Somya, James M McCaw, Mark B Flegg, Peter G Taylor, and Jennifer A Flegg (2020). “An Activation-Clearance Model for *Plasmodium vivax* Malaria”. In: *Bulletin of Mathematical Biology* 82.2, p. 32.
- Price, Ric N, Robert J Commons, Katherine E Battle, Kamala Thriemer, and Kamini Mendis (2020). “*Plasmodium vivax* in the Era of the Shrinking *P. falciparum* Map”. In: *Trends in Parasitology*.

WHO (2020). *World malaria report 2020: 20 years of global progress and challenges*. World Health Organization.

Mehra, Somya, James M McCaw, Mark B Flegg, Peter G Taylor, and Jennifer A Flegg (2021). “Antibody Dynamics for Plasmodium vivax Malaria: A Mathematical Model”. In: *Bulletin of Mathematical Biology* 83.1, pp. 1–27.